NUREG/IA-0222

International Agreement Report

Analysis of RELAP5/MOD3.3 Prediction of 2-Inch Loss-of-Coolant Accident at Krško Nuclear Power Plant

Prepared by:
I. Parzer, B. Mavko

Jožef Stefan Institute
Jamova cesta 39
SI-1000 Ljubljana, Slovenia

A. Calvo, NRC Project Manager

Office of Nuclear Regulatory Research
U.S. Nuclear Regulatory Commission
Washington, DC 20555-0001

March 2010

Prepared as part of
The Agreement on Research Participation and Technical Exchange
Under the Thermal-Hydraulic Code Applications and Maintenance Program (CAMP)

Published by
U.S. Nuclear Regulatory Commission

AVAILABILITY OF REFERENCE MATERIALS IN NRC PUBLICATIONS

NRC Reference Material

As of November 1999, you may electronically access NUREG-series publications and other NRC records at NRC's Public Electronic Reading Room at http://www.nrc.gov/reading-rm.html. Publicly released records include, to name a few, NUREG-series publications; *Federal Register* notices; applicant, licensee, and vendor documents and correspondence; NRC correspondence and internal memoranda; bulletins and information notices; inspection and investigative reports; licensee event reports; and Commission papers and their attachments.

NRC publications in the NUREG series, NRC regulations, and *Title 10, Energy*, in the Code of *Federal Regulations* may also be purchased from one of these two sources.

1. The Superintendent of Documents
   U.S. Government Printing Office
   Mail Stop SSOP
   Washington, DC 20402–0001
   Internet: bookstore.gpo.gov
   Telephone: 202-512-1800
   Fax: 202-512-2250
2. The National Technical Information Service
   Springfield, VA 22161–0002
   www.ntis.gov
   1–800–553–6847 or, locally, 703–605–6000

A single copy of each NRC draft report for comment is available free, to the extent of supply, upon written request as follows:

Address: U.S. Nuclear Regulatory Commission
Office of Administration
Reproduction and Mail Services Branch
Washington, DC 20555-0001
E-mail: DISTRIBUTION@nrc.gov
Facsimile: 301–415–2289

Some publications in the NUREG series that are posted at NRC's Web site address http://www.nrc.gov/reading-rm/doc-collections/nuregs are updated periodically and may differ from the last printed version. Although references to material found on a Web site bear the date the material was accessed, the material available on the date cited may subsequently be removed from the site.

Non-NRC Reference Material

Documents available from public and special technical libraries include all open literature items, such as books, journal articles, and transactions, *Federal Register* notices, Federal and State legislation, and congressional reports. Such documents as theses, dissertations, foreign reports and translations, and non-NRC conference proceedings may be purchased from their sponsoring organization.

Copies of industry codes and standards used in a substantive manner in the NRC regulatory process are maintained at—

The NRC Technical Library
Two White Flint North
11545 Rockville Pike
Rockville, MD 20852–2738

These standards are available in the library for reference use by the public. Codes and standards are usually copyrighted and may be purchased from the originating organization or, if they are American National Standards, from—

American National Standards Institute
11 West 42nd Street
New York, NY 10036–8002
www.ansi.org
212–642–4900

Legally binding regulatory requirements are stated only in laws; NRC regulations; licenses, including technical specifications; or orders, not in NUREG-series publications. The views expressed in contractor-prepared publications in this series are not necessarily those of the NRC.

The NUREG series comprises (1) technical and administrative reports and books prepared by the staff (NUREG–XXXX) or agency contractors (NUREG/CR–XXXX), (2) proceedings of conferences (NUREG/CP–XXXX), (3) reports resulting from international agreements (NUREG/IA–XXXX), (4) brochures (NUREG/BR–XXXX), and (5) compilations of legal decisions and orders of the Commission and Atomic and Safety Licensing Boards and of Directors' decisions under Section 2.206 of NRC's regulations (NUREG–0750).

DISCLAIMER: This report was prepared under an international cooperative agreement for the exchange of technical information. Neither the U.S. Government nor any agency thereof, nor any employee, makes any warranty, expressed or implied, or assumes any legal liability or responsibility for any third party's use, or the results of such use, of any information, apparatus, product or process disclosed in this publication, or represents that its use by such third party would not infringe privately owned rights.

NUREG/IA-0222

International Agreement Report

Analysis of RELAP5/MOD3.3 Prediction of 2-Inch Loss-of-Coolant Accident at Krško Nuclear Power Plant

Prepared by:
I. Parzer, B. Mavko

Jožef Stefan Institute
Jamova cesta 39
SI-1000 Ljubljana, Slovenia

A. Calvo, NRC Project Manager

Office of Nuclear Regulatory Research
U.S. Nuclear Regulatory Commission
Washington, DC 20555-0001

March 2010

Prepared as part of
The Agreement on Research Participation and Technical Exchange
Under the Thermal-Hydraulic Code Applications and Maintenance Program (CAMP)

Published by
U.S. Nuclear Regulatory Commission

ABSTRACT

The purpose of this analysis was to perform calculations of the loss-of-coolant accident (LOCA) for simulator verification and validation and to study the thermal-hydraulic response of the reactor coolant system.

For the thermal-hydraulic analysis, the RELAP5/MOD3.3 code and input model provided by Krško Nuclear Power Plant was used. A small-break LOCA scenario was analyzed to estimate plant response to the opening of a break in cold leg No. 2 between the reactor coolant pump and the reactor pressure vessel. For the purpose of the analysis, the equivalent diameter of the cross-sectional area of the break was set to 5.08 centimeters (2 inches).

In the presented study, the 2-inch LOCA scenario for the Krško Nuclear Power Plant was analyzed with regard to the differences between the Henry-Fauske and the Ransom-Trapp critical flow model. In addition, the study investigated the effect of the special offtake flow model at the break. Some variation cases were also run to capture the effect of flow bypasses in the reactor vessel on the loop seal clearing phenomena.

CONTENTS

Figures

Tables

ACKNOWLEDGEMENT

The RELAP5/MOD3.3 NPP Krško base input model and nodalization diagram are courtesy of Krško Nuclear Power Plant.

ABBREVIATIONS

AFW	auxiliary feedwater
CPU	central processing unit
ECCS	emergency core cooling system
H-F	Henry-Fauske
HPIS	high-pressure injection system
KFSS	Krško full-scope simulator
kg/s	kilogram per second
LOCA	loss-of-coolant accident
LPIS	low-pressure injection system
m	meter
MCR	main control room
MFW	main feedwater
mm	millimeter
MPa	megapascal
MWt	megawatt thermal
NPP	nuclear power plant
PRZ	pressurizer
PWR	pressurized-water reactor
RAM	random access memory
RCS	reactor coolant system
RCP	reactor coolant pump
RPV	reactor pressure vessel
R-T	Ransom-Trapp
s	second
SI	safety injection
SG	steam generator

1. INTRODUCTION

Krško Nuclear Power Plant (NPP) obtained the Krško full-scope simulator (KFSS) as part of the modernization project in 1999. KFSS supports, in real time, training for the complete range of operation which can be performed from the main control room (MCR) and some selected plant areas (e.g., remote shutdown panels).

Various activities have been undertaken for the purpose of simulator annual verification. Initially, these activities included simulator verification for the normal plant operation (normal power evolutions, plant heatup and cooldown), plant transients, and steady-state conditions at different power levels. The data recorded in the past and obtained from the MCR instrumentation and process information system were used.

When conducting the simulator annual verification for selected design-basis accidents and certain transients, it is important to use the results of the best estimate analysis. This approach complies with American National Standards Institute/American Nuclear Society (ANSI/ANS)-3.5-1998, "Nuclear Power Plant Simulators for Use in Operator Training and Examination (Revision of ANSI/ANS-3.5-1993 and ANSI/ANS-3.5-1985)" (Ref. 1).

The purpose of the present analysis was to perform loss-of-coolant accident (LOCA) calculations for verification and validation using the KFSS and to study the thermal-hydraulic response of the reactor coolant system (RCS) (Ref. 2).

Several analyses during the past few years have proved that the original Ransom-Trapp break flow model has certain deficiencies and its predictions do not match experimental data. Thus, the older Henry-Fauske (H-F) break model has been again coded into RELAP5/MOD3. At first, the H-F model was an option, and the Ransom-Trapp (R-T) model was considered the main prediction tool. A longer testing period has established that the H-F model performs better for various test cases; it is now the main modeling tool in the code. The R-T model remains as a user option in the code.

During the assessment program for the application of the RELAP5 code to Westinghouse's proposed advanced passive design (i.e., the AP600), the following two shortcomings of the default R-T choking model were observed:

(1) Two-Phase Critical Flow at Low Pressure: If the slip ratio is not forced to be nearly unity, the values calculated using the default choking model could be as much as an order of magnitude lower than the homogeneous equilibrium values.

(2) Subcooled Break Flow: For thin orifice plates (used to model the break) and liquid conditions near the saturation point, the default choking model predicted values of the critical flow were 40–50 percent less than those observed experimentally.

The most serious shortcoming occurred at low pressure (P ~ 2 bar) and low quality conditions. Another significant, but less serious, shortcoming of the default critical flow model was observed when the experimental break configuration was a thin orifice plate (t ~ 10 millimeters (mm)) and the flow was slightly subcooled.

In addition to the shortcomings discussed above, several users have reported problems, noting apparent discontinuities in the predicted critical flow values for the single-phase to two-phase transition and the appearance of a noncondensable gas in a two-phase mixture. Several users have also reported that the default critical flow model predicted values that were considerably "noisier" than those predicted by earlier versions of RELAP5 employing the H-F critical flow model. For these reasons, a modified form of the H-F critical flow model was reintroduced into the RELAP5 code.

In the present study, the 2-inch LOCA scenario for the Krško NPP was analyzed with regard to the differences between the H-F and R-T critical flow models. The effect of the special offtake flow model at the break was also investigated. Some variation cases were run to capture the effect of flow bypasses in the reactor vessel on the loop seal clearing phenomena.

2. PLANT DESCRIPTION

Krško NPP is a Westinghouse two-loop pressurized-water reactor (PWR) plant with a large dry containment. The plant has been in commercial operation since 1983. After modernization in 2000, the plant's fuel cycle was gradually prolonged from 12 (cycle 17) to 18 months (cycle 21).

The power rating of the Krško NPP nuclear steam supply system is 2,000 megawatt thermal (MWt) (1,882 MWt before the plant modernization and power uprate), comprising 1,994 MWt (1,876 MWT before the plant modernization and power uprate) of core power output plus 6 MWt of reactor coolant pump (RCP) heat input. The nuclear steam supply system consists of a PWR, RCS, and associated auxiliary fluid systems. The RCS is arranged as two closed reactor coolant loops connected in parallel to the reactor vessel, each containing an RCP and a steam generator (SG). An electrically heated pressurizer is connected to one of the loops.

The reactor core is composed of 121 fuel assemblies. Square spacer grid assemblies and the upper and lower end fitting assemblies support the fuel rods in fuel assemblies. Each fuel assembly is composed of 16 x 16 rods; of these, only 235 places are used by fuel rods. Of the 21 remaining places, 20 are evenly and symmetrically distributed across the cross-section of the assembly and are provided with thimble tubes which may be reserved for control rods and one control instrumentation tube for in-core thimble.

The RCPs, one per coolant loop, are Westinghouse vertical, single-stage, centrifugal pumps of the shaft-seal type.

The SGs, one per loop, are vertical U-tube, Siemens-Framatome type SG 72 W/D4-2 units, installed during the plant modernization in 2000. These new SGs replaced highly degraded Westinghouse D-4 SGs, each having preheating section.

Engineered safety features are provided to prevent accident propagation, or to limit the consequences of postulated accidents, which might otherwise lead to damage of the system and release of fission products. The plant includes a number of engineered safety features, which include the following:

- containment spray system
- hydrogen control system
- emergency core cooling system (ECCS)
- component cooling water system
- essential service water system
- auxiliary feedwater system

At present, activities are underway to replace the turbine and to gain additional power from new SGs.

3. THEORETICAL BACKGROUND

3.1 Ransom-Trapp Model

The two-phase choking model employed in RELAP5 is based on the model described by Trapp and Ransom (Ref. 3) for nonhomogeneous, nonequilibrium flow. These researchers developed analytic choking criteria using a characteristic analysis of a two-fluid model that included relative phasic acceleration terms and derivative-dependent mass transfer. During the original development and implementation of this model, both frozen flow and thermal equilibrium assumptions were employed to test the analytic criteria. Comparisons to existing data (Ref. 4) indicated that the thermal equilibrium assumption was the more appropriate and is thus assumed in the following development.

The two-fluid model employed in the development of the RELAP5 two-phase choking criteria includes an overall mass conservation equation, two-phasic momentum equations, and the mixture energy equation written in terms of entropy. This equation set includes interface force terms due to relative acceleration; these terms have a significant effect on wave propagation. Energy dissipation terms associated with interface mass transfer and relative phase acceleration have been neglected in the mixture entropy equation. The characteristic velocities of the system of equations are the roots (λ_i, $i < 4$) of the characteristic polynomial:

$$A\lambda - B = 0 \tag{1}$$

The real part of any root λ_i gives the velocity of signal propagation along the corresponding path in the space/time plane. If the defined system of equations is considered for a particular region defined by $0 < x < L$, the number of boundary conditions required at L equals the number of characteristic lines entering the solution region. At $x = L$, as long as any of the λ_i are less than 0, some information is needed at the boundary to get a solution. If all λ_i are greater than or equal to 0, no boundary conditions are needed at L and the solution of $0 < x < L$ is not affected by conditions outside the boundary at L. This situation defines the choking criteria:

$$\lambda_j = 0 \text{ for } j \le 4 \quad \text{and} \quad \lambda_j \ge 0 \text{ for all } i \ne j \tag{2}$$

Reference 1 provides further detailed derivation of the choking criteria.

3.2 Henry-Fauske Model

The steady-state, one-dimensional momentum equation for one-component, two-phase flow can be written as follows:

$$-AdP = d(\dot{m}_v u_v + \dot{m}_l u_l) + dF_w \tag{3}$$

For high-velocity flows in a converging nozzle, the wall shear forces are negligible compared to the momentum and pressure gradient terms, allowing the mass flux at the throat to be approximated by the following equation:

$$G = -\left\{ \frac{d\left[xu_v + (1-x)u_l\right]}{dP} \right\}_t \tag{4}$$

At critical flow, the mass flow rate exhibits a maximum with respect to the throat pressure. Equations (3) and (4) can be combined to give the following expression for the critical flow rate for an isentropic homogeneous mixture with flashing:

$$G_c^2 = \frac{-1}{\left\{ x\frac{\partial v_v}{\partial P} + (1-x)\frac{\partial v_l}{\partial P} + (v_v - v_l)\frac{\partial x}{\partial P}\bigg|_s \right\}_t} \tag{5}$$

Embedded in this equation is the assumption that the two phases move with the same velocity; that is, that the slip ratio is unity. While at low pressure, this is certainly not the case. Henry and Fauske argued that the effects of thermal nonequilibrium were more important and that the effect of slip could be ignored. Equation (5) then serves as the choking criterion; however, to evaluate the critical mass flux, the quantities in this expression must be evaluated at the local conditions occurring at the throat. Thus, it is assumed that the phase velocities are equal. For normal nozzle configurations, there is little time for mass transfer to take place, and it is reasonable to assume that the amount of mass transferred during the expansion is negligible. Similarly, the amount of heat transferred between the phases during the expansion is also negligible, so that the liquid temperature is essentially constant. Since wall shear, heat transfer with the environment, and interfacial viscous terms were neglected, the system entropy during the expansion was assumed constant.

The above assumptions eliminate the need to calculate the liquid-specific volume and the quality at the throat and also provide a relation for the vapor-specific volume in terms of the throat pressure and the upstream conditions. Evaluation of the throat pressure and the three differential terms remains. Putting all of the above assumptions into Equation (5), the final expression for the critical value of the mass flux is further determined in Reference 1.

3.3 Phase Separation and Offtake Model

Phase separation usually results from gravitational forces, which cause the liquid phase to pool at the bottom of a vertical volume or on the bottom of a large horizontal pipe. This can occur if the flow rates of the phases in the volume are low enough so that gravitational forces overcome the frictional force between the phases that tends to keep the phases well mixed. The phase separation caused by gravitational forces is called flow stratification in RELAP5, and both the vertical and horizontal flow regime maps show stratification regions (Ref. 1).

One consequence of stratification in a large horizontal pipe is that the properties of the fluid convected through a small flowpath in the pipe wall (i.e., a small break), called an offtake, depend on the location of the stratified liquid level in the large pipe relative to the location of the flowpath in the pipe wall. If the offtake is located in the bottom of the horizontal pipe, liquid will flow through the offtake until the liquid level starts to approach (but not reach) the bottom of the pipe, at which time some vapor will be pulled through the liquid layer and the fluid quality in the offtake will increase. If the phase separation phenomenon is ignored, vapor will be passed through the offtake regardless of the liquid level in the pipe. Likewise, if the offtake is located at the top of the pipe, vapor will be convected through the offtake until the liquid level rises high

enough so that liquid can be entrained from the stratified surface. The flow quality in the offtake will decrease as the liquid level rises. If the phase separation phenomenon is ignored, liquid will pass through the offtake for all stratified liquid levels regardless of their height relative to the offtake. Lastly, if the offtake is located in the side of the large horizontal pipe, the same phenomenon of gas pullthrough or liquid entrainment will occur, depending on the elevation of the stratified liquid level in the pipe relative to the location of the offtake in the wall of the pipe (Ref. 1).

The results of the experiments showed that in most cases the depth or height (i.e., the distance between the stratified liquid level and the elevation of the offtake) for the onset of liquid entrainment or gas pullthrough could be defined by an equation of the following form (Ref. 1):

$$h_b = \frac{CW_k^{0.4}}{\left[g\rho_k\left(\rho_f - \rho_g\right)\right]^{0.2}} \tag{6}$$

where subscript k refers to the continuous phase in the offtake, which is the phase flowing through the offtake before the onset of pullthrough or entrainment of the other phase. For an upward offtake, the gas phase is the continuous phase. For a downward offtake, the liquid phase is the continuous phase. For a side offtake, the gas phase is the continuous phase when the liquid level is below the offtake center, and the liquid phase is the continuous phase when the liquid level is above the offtake center. The variable W_k is the mass flow rate of the continuous phase in the offtake.

For the specific case of a 2-inch LOCA at Krško NPP, a variation case was calculated for each analyzed break model (H-F and R-T), in which the break was situated at the side of the cold leg between the RCP and reactor vessel. Each time, the side offtake model was assumed. Based on the experimental studies, it may be concluded that the use of Equation (6) should give a reasonable representation of the test data if the following values are adopted for the correlation constant C (Ref. 1):

- C = 0.75 for side offtake gas pullthrough
- C = 0.69 for side offtake liquid entrainment

The correlation for the flow quality through a side offtake has the following form (Ref. 1):

$$X = X_o^{(1+CR)}\left[1 + 0.5R(1+R)X_o^{(1-R)}\right]^{0.5} \tag{7}$$

where

$$X_o = \frac{1.15}{1+\sqrt{\rho_f/\rho_g}} \quad \text{and} \quad R = \frac{h}{h_b} \tag{8}$$

In Equation (7), C = 1.09 for gas pullthrough and C = 1.00 for liquid entrainment.

4. INPUT MODEL DESCRIPTION

To perform this analysis, Krško NPP provided the base input model or "master input deck," which is described in Krško NPP proprietary documents (Refs. 5 and 6). Figure 1 presents the scheme of the Krško NPP nodalization for the RELAP5/MOD3.3 code (Ref. 1). A full two-loop plant model was developed, including the new Siemens-Framatome type SG 72 W/D4-2 replacement SGs.

The model consists of 469 volumes, connected with 497 junctions. Plant structure is represented by 376 heat structures with 2,101 mesh points. The reactor protection and regulation systems and the safety systems' operational logic and plant instrumentation is represented by 401 logical conditions (trips) and 575 control variables.

4.1 Hydrodynamic Component Description

Components numbered from 101 to 165 represent the reactor vessel in the following manner:

171, 173, and 175	lower downcomer
101 and 103	lower head
105	lower plenum
107	core inlet
111	reactor core
115	core baffle bypass
121	core outlet
125, 131, and 141	upper plenum
151 and 153	upper head
165	upper downcomer
113 and 145	guide tubes

Components numbered 51, 53, and 55 represent the pressurizer surge line and volumes 61, 63, 65, 67, and 69 represent the pressurizer vessel. Pressurizer spray lines (80, 81, and 84) are connected to the top of the pressurizer vessel and include the spray valves numbered 82 and 83. Valves numbered 28 and 32 represent the two pressurizer power-operated relief valves and valves numbered 14 and 22 represent pressurizer safety valves.

Primary piping is represented by the following components:

201, 203, 205, 207, 209, and 211	hot leg No. 1
251, 253, 255, 257, and 259	intermediate leg No. 1 with cold leg No. 1 loop seal
265, 271, 273, 275, 277, and 279	cold leg No. 1 with the primary coolant pump No. 1
301, 303, 305, 307, 309, and 311	hot leg No. 2
351, 353, 355, 357, and 359	intermediate leg No. 2 with cold leg No. 2 loop seal
365, 371, 373, 375, 377, and 379	cold leg No. 2 with the primary coolant pump No. 2

Loops are symmetrical except for the pressurizer surge line and chemical and volume control system connections layout.

Hydrodynamic components numbered from 701 to 882 represent the ECCS piping nodalization

and connections. The hydrodynamic components representing the high-pressure injection system (HPIS) pumps are time-dependent junctions 703 and 803, and time-dependent junctions 750 and 850 represent the low-pressure injection system (LPIS) pumps. Accumulators are numbered 701 and 801, and their lineup provides cold-leg injection only. The ECCS connects to both cold legs (junctions 719-01 and 819-01). Direct vessel ECCS injection through junctions 746 and 748 opens simultaneously upon generation of a safety injection (SI) signal.

The primary side of the SG is represented by inlet and outlet plenum, among which a single pipe represents the U-tube bundle, as follows:

215, 217, and 219	SG 1 inlet plenum (hot side) and tubesheet inlet
223, 225, 227, 233, 235, and 237	SG 1 U-tubes
241, 243, and 245	SG 1 tubesheet outlet and outlet plenum (cold side)
315, 317, and 319	SG 2 inlet plenum (hot side) and tube sheet inlet
323, 325, 327, 333, 335, and 337	SG 2 U-tubes
341, 343, and 345	SG 2 tubesheet outlet and outlet plenum (cold side)

The following hydrodynamic components represent the parts of the SG secondary side:

415, 417, and 419	SG 1 riser
421 and 427	SG 1 separator and separator pool
411 and 413	SG 1 downcomer
423, 425, and 429	SG 1 steam dome
515, 517, and 519	SG 2 riser
521 and 527	SG 2 separator and separator pool
511 and 513	SG 2 downcomer
523, 525, and 529	SG 2 steam dome

The main steamlines are represented by volumes 451, 453, 455, 457, 459, and 461 (SG 1) and 551, 553, 555, 557, 559, and 561 (SG 1), divided by main steam isolation valves (458 and 558). SG relief (482 and 582) and safety valves (484, 486, 488, 492, and 494 and 584, 586, 588, 592, and 594) are situated upstream of the isolation valves. Turbine valve (604) and steam dump (611) flow is regulated by corresponding logic.

The main feedwater (MFW) piping is represented by volumes 471, 473, 475, 407, and 409 (SG 1) and 471, 573, 575, 507, and 509 (SG 2), branching from the MFW header (500).

Auxiliary feedwater (AFW) is injected above the SG riser (via volumes 437, 443, 445, and 447), and its piping is represented by volumes 671, 673 (motor-driven AFW 1), 675 and 677 (AFW 2), and 681, 683, 685, 687, 695, and 697 (turbine-driven AFW).

4.2 Regulation and Protection Logic

To accurately represent the Krško NPP behavior, the model includes a considerable number of control variables and general tables. These represent the protection, monitoring, and simplified control systems used only during steady-state initialization, as well as the following main plant control systems:

- rod control system
- pressurizer pressure control system
- pressurizer level control system
- SG level control system
- steam dump

The rod control system has been modeled for point kinetics. The present model can be used for transient analysis with either of the following two options:

(1) with constant or predefined core power transient as a function of time (including decay power calculation)

(2) with rod control system in auto or manual mode

The following plant protection systems are defined using trip logic:

- reactor trip
- SI signal
- turbine trip
- steamline isolation
- MFW isolation
- AFW start

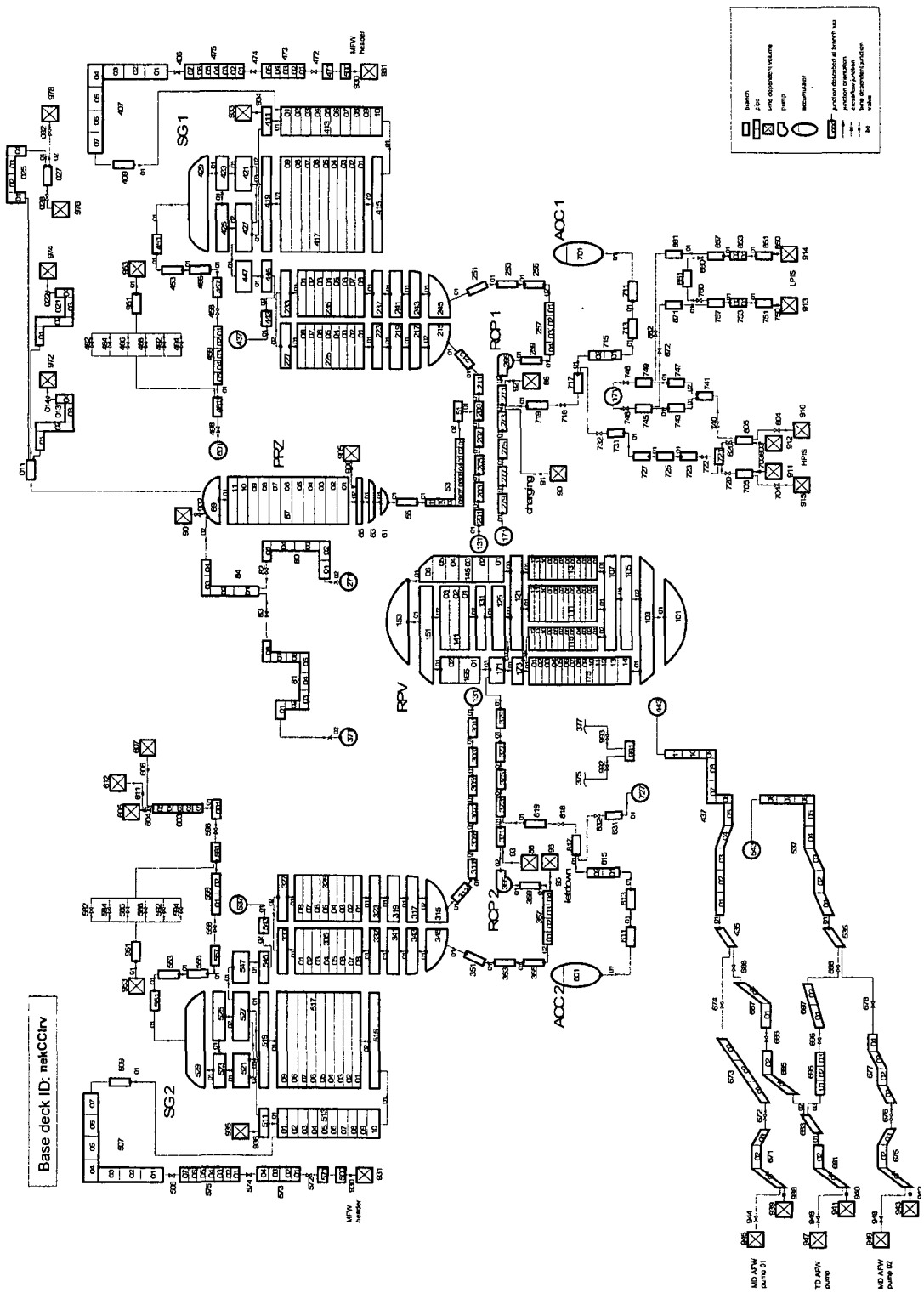

Figure 1 Krško NPP nodalization scheme

5. RESULTS

5.1 Base Analyses—Comparison of Critical Flow Models

This set of analyses evaluated the differences between the default H-F and the R-T critical flow models.

After the break occurred, the primary system started draining and the pressurizer pressure dropped very quickly to the saturation pressure of the hot legs. The pressurizer emptied (Figure 2) in 34 seconds using the H-F model and in 30 seconds using the R-T model after the break opening and stayed empty. Primary pressure (Figure 3) is one of the most important parameters during a small-break LOCA event, since it dictates the tripping sequence and many setpoints used in the analysis. The reactor was tripped when the filtered primary pressure (LEAD-LAG) dropped below 12.994 megapascals (MPa).

An SI signal was produced when the primary pressure dropped to 12.27 MPa. Soon after that, the HPIS pumps started to deliver cold borated water into the primary system, reaching the break location. At the point where the highly subcooled liquid entered the break, the R-T model calculated a significantly higher break flow (Figure 4) than did the default H-F model. As a consequence, the primary inventory (Figure 5) was depleted much faster in the R-T case than in the default H-F case. This led to further important differences in the transient predictions.

The power produced in the core was transferred out of the primary system; therefore, both hot-leg temperatures decreased. At the beginning of the transient, the temperatures of the cold legs (Figures 6 and 7) decreased because of a pressure drop of the primary system to the saturation temperature. Later, the cold-leg temperatures followed the loop seal behavior. When the loop seal was cleared, the cold-leg temperature suddenly dropped; when the loop seal refilled, the temperature increased.

Initially after the reactor trip, the MFW was isolated and the turbine valves were closed. Closure of the turbine valves caused a shrink effect. The heat generated in the core started to heat the SGs. The heat input caused the pressure in the SGs (Figures 8 and 9) to increase. Later, the AFW pumps started to inject the cold water into the SGs, which then started to cool. When the SG narrow range levels (Figures 10 and 11) reached 72 percent, the AFW pumps were stopped and the SG pressures stabilized 1,000 seconds later.

The closure of the turbine valves caused the SG narrow range levels (Figures 10 and 11) to shrink. Both levels increased when the AFW pumps started to inject into the SGs.

When the primary pressure reached 4.96 MPa, the accumulators started to inject. As the accumulators discharged, the accumulator pressure (Figures 12 and 13) decreased. The accumulators (Figures 14 and 15) were not emptied by the end of calculation time in the H-F case. This phenomenon happened much earlier in the R-T case.

The core partly uncovered (Figure 16) because of the loop seal formation (Figures 17, 18, 19, and 20). When the loop seal was first cleared, the liquid in the downcomer refilled the core. Later, the core stayed partially uncovered and the core level oscillated slightly because the cold water injected from the accumulator into the cold leg and downcomer evaporated in the core.

The generated steam increased the pressure, which reduced the accumulator flow.

Rather unphysical oscillations in primary pressure were observed during multiple loop seal clearings. One possible explanation is that primary pressure spikes were in the range of 2 MPa, while the pressure difference needed to clear a loop seal of approximate 3 meters in height should not exceed 0.025 MPa. Observing the pressure difference on both sides of the loop seal (Figure 21) provides more detailed insight into the phenomena. It can be deduced that the HPIS injection flow caused the main pressure rise. Since the upper parts of the system had emptied by the time of the first loop seal clearing, pressure spikes could propagate through the reactor vessel upper head bypass, empty hot legs, and SG tubes to the SG side of the loop seal. Thus, the additional pressure rise resulting from vapor generation in the core, which was the origin of the driving force for the loop seal clearing, was only superposed to the main pressure spike. This pressure was only about 0.03 MPa, as can be estimated from Figure 21.

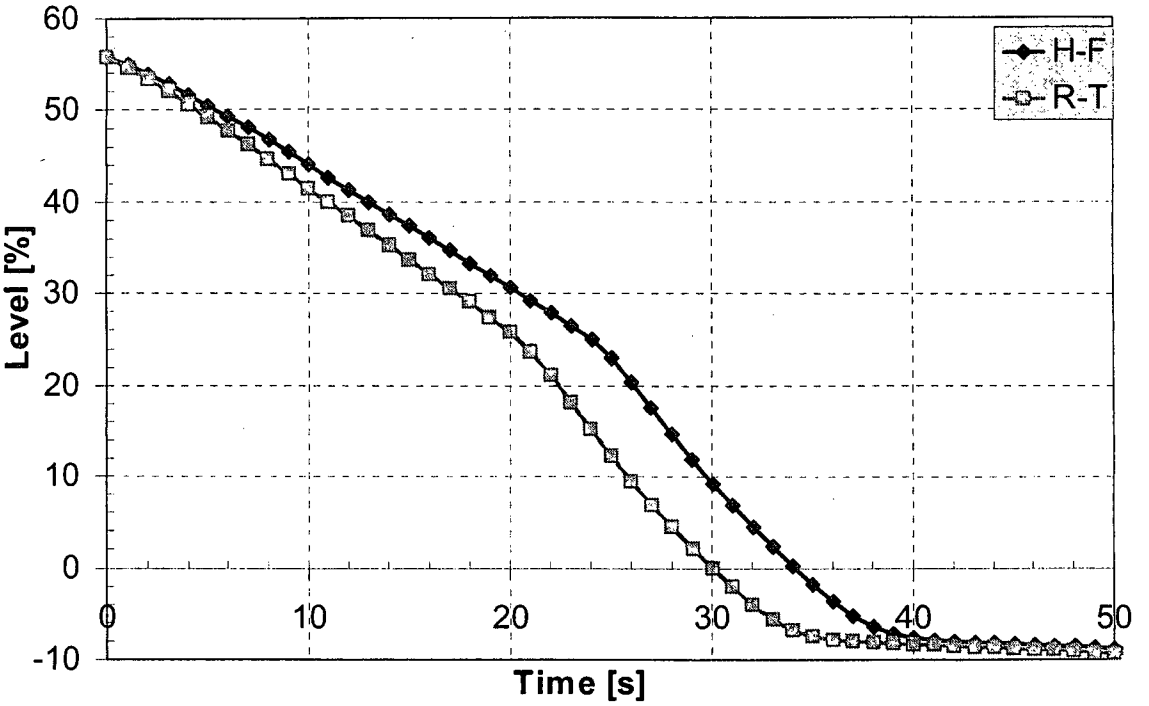

Figure 2 PRZ level

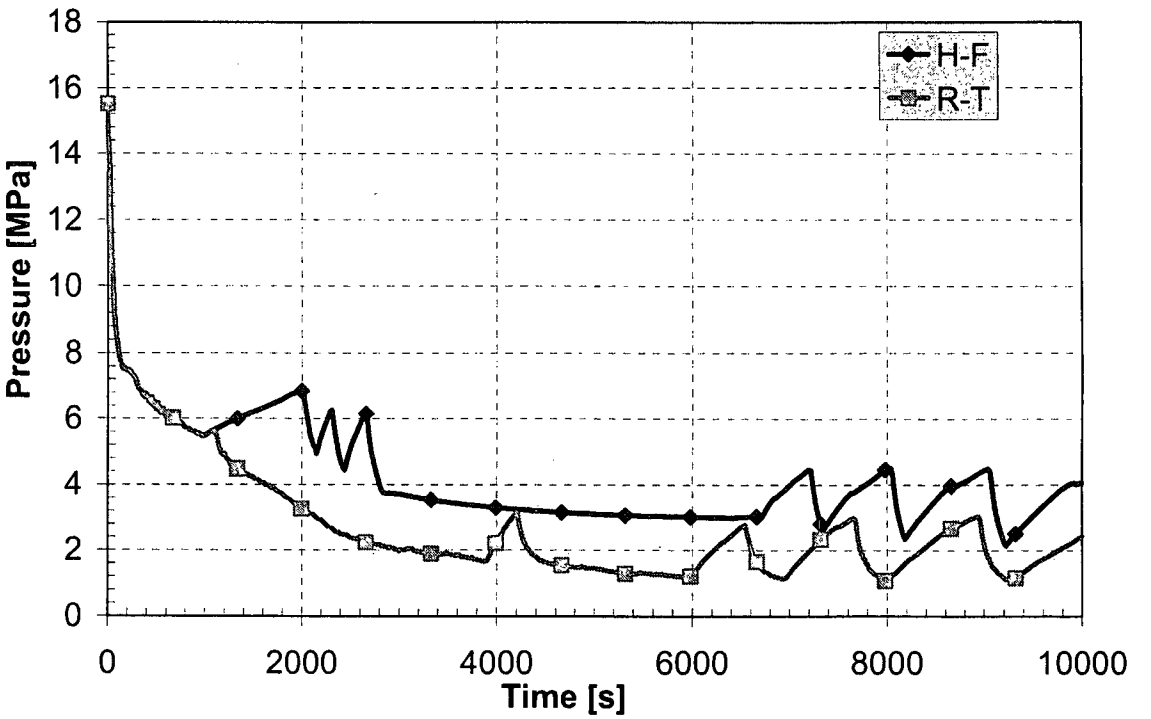

Figure 3 PRZ pressure

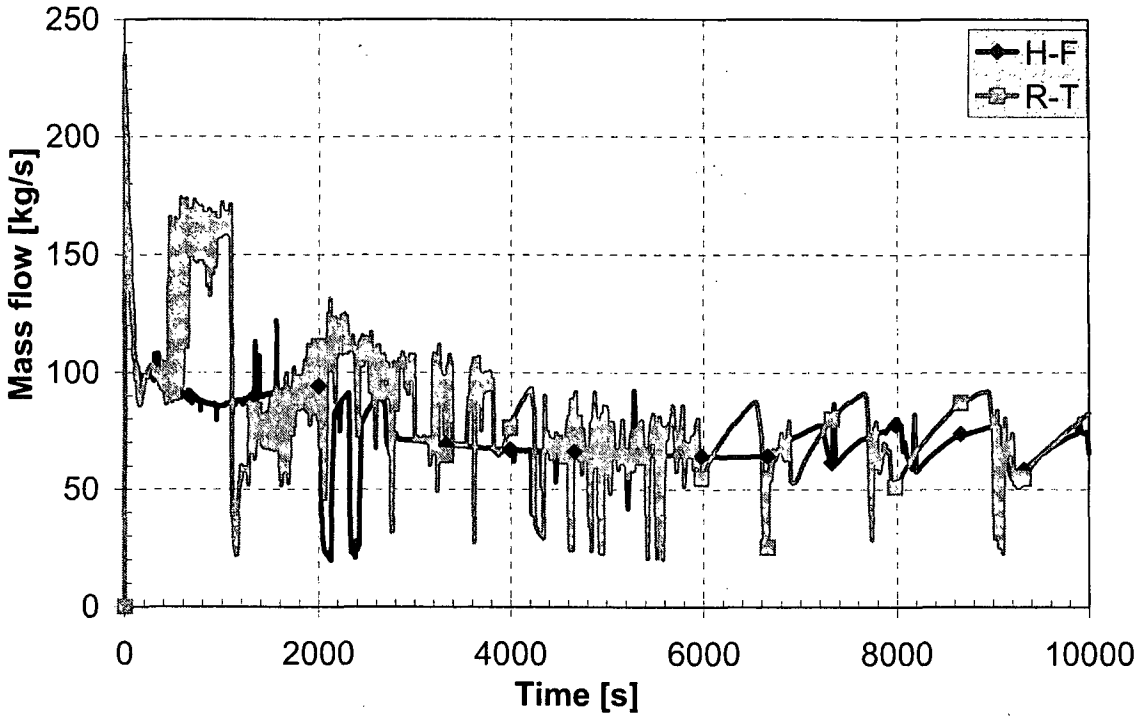

Figure 4 Break flow

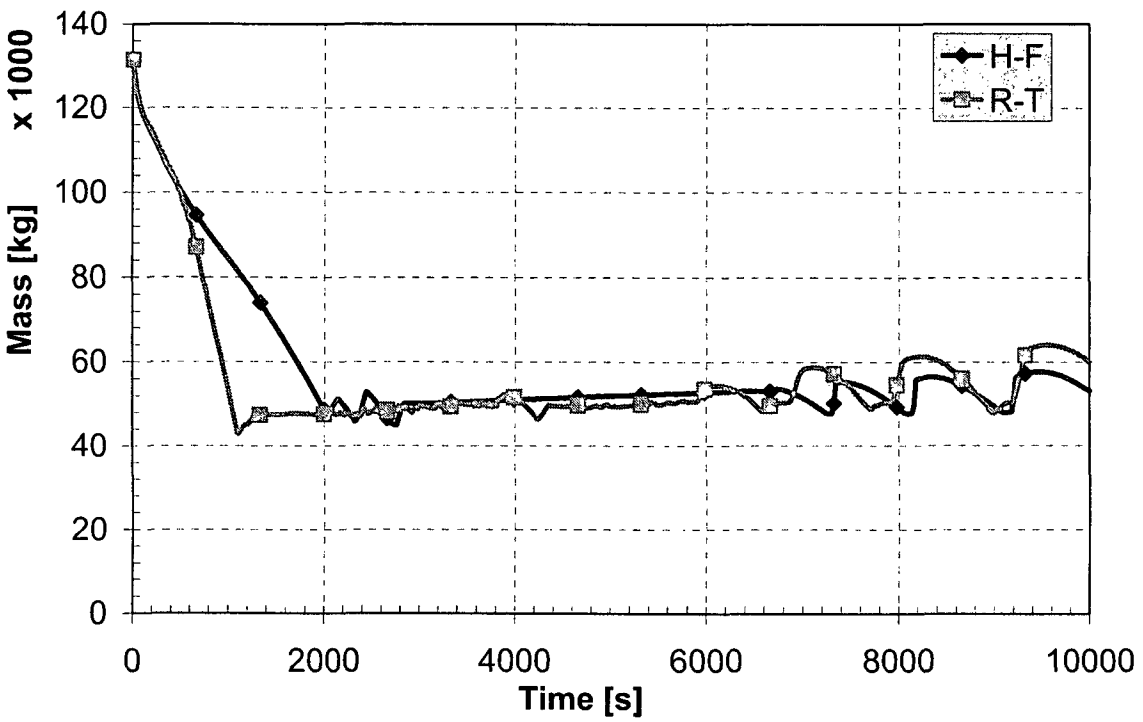

Figure 5 Primary mass

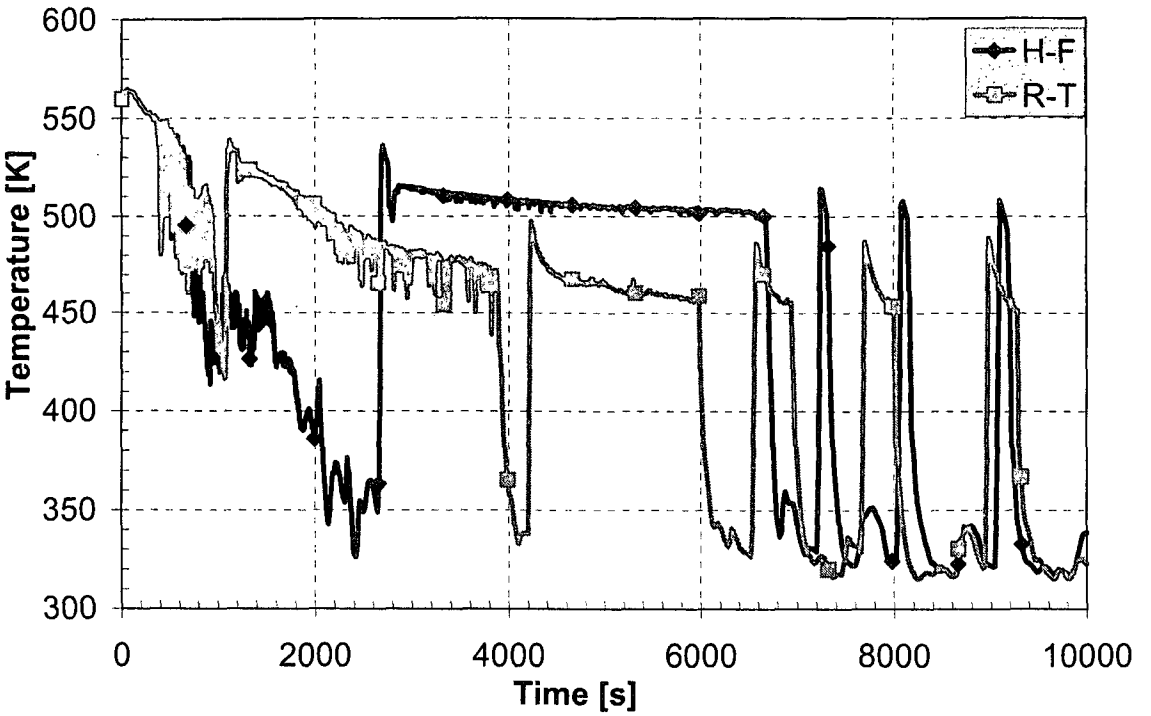

Figure 6 Cold leg No. 1 temperature

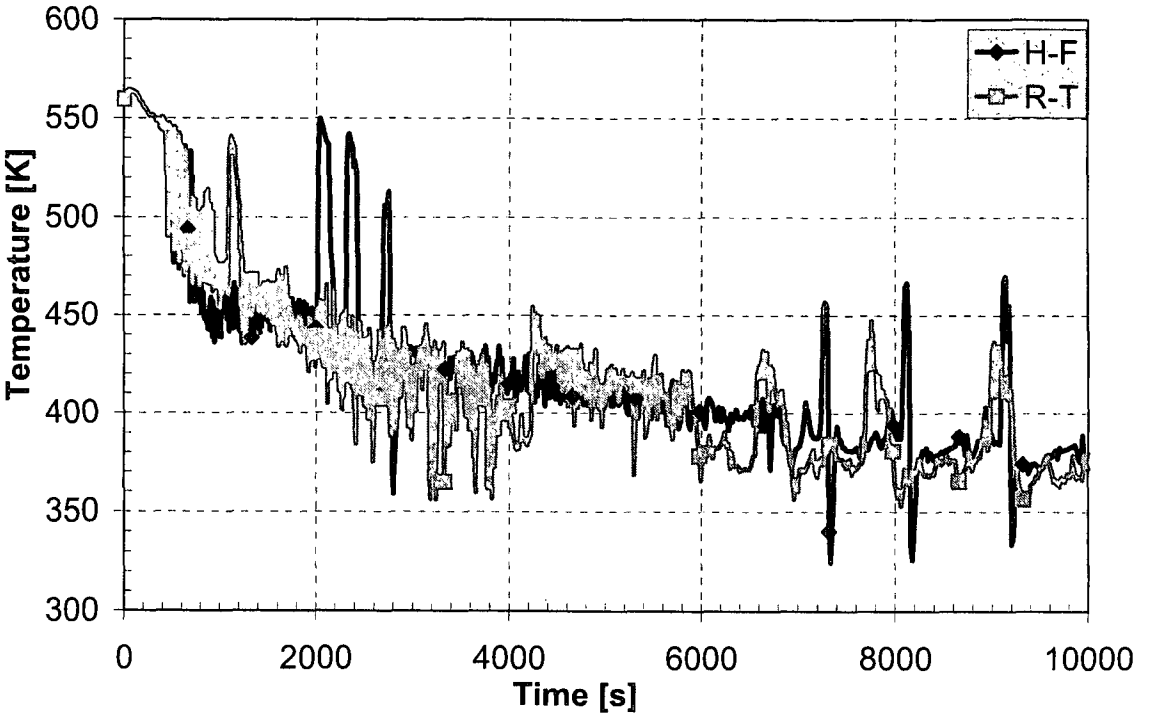

Figure 7 Cold leg No. 2 temperature

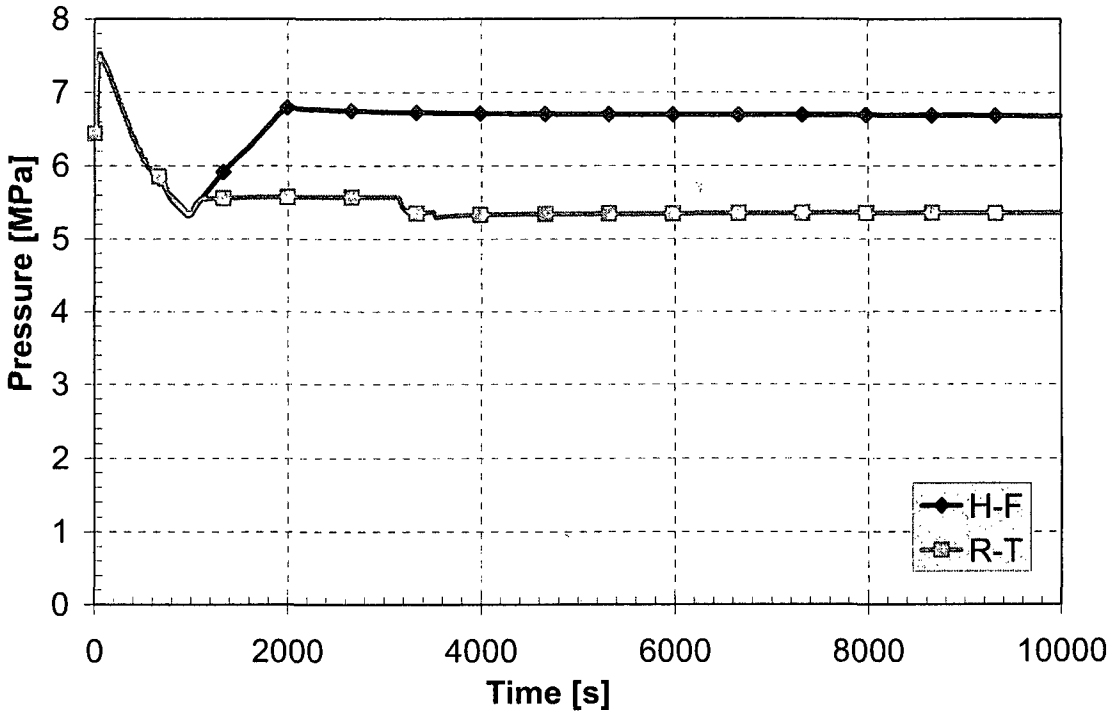

Figure 8 SG 1 pressure

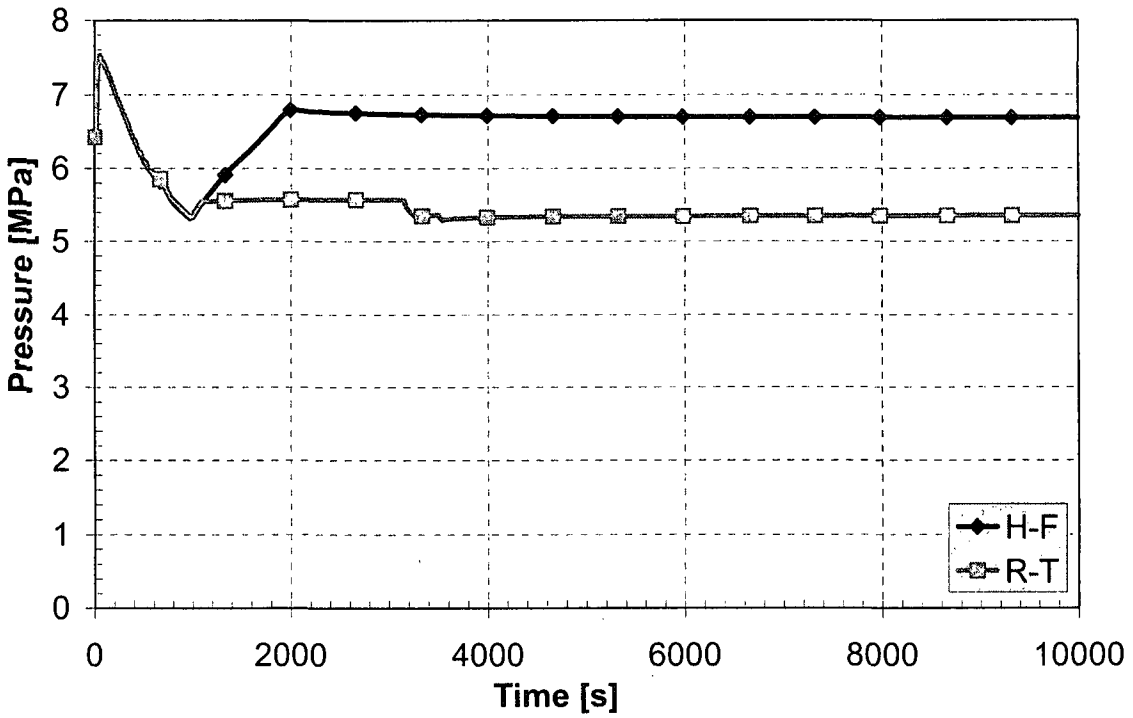

Figure 9 SG 2 pressure

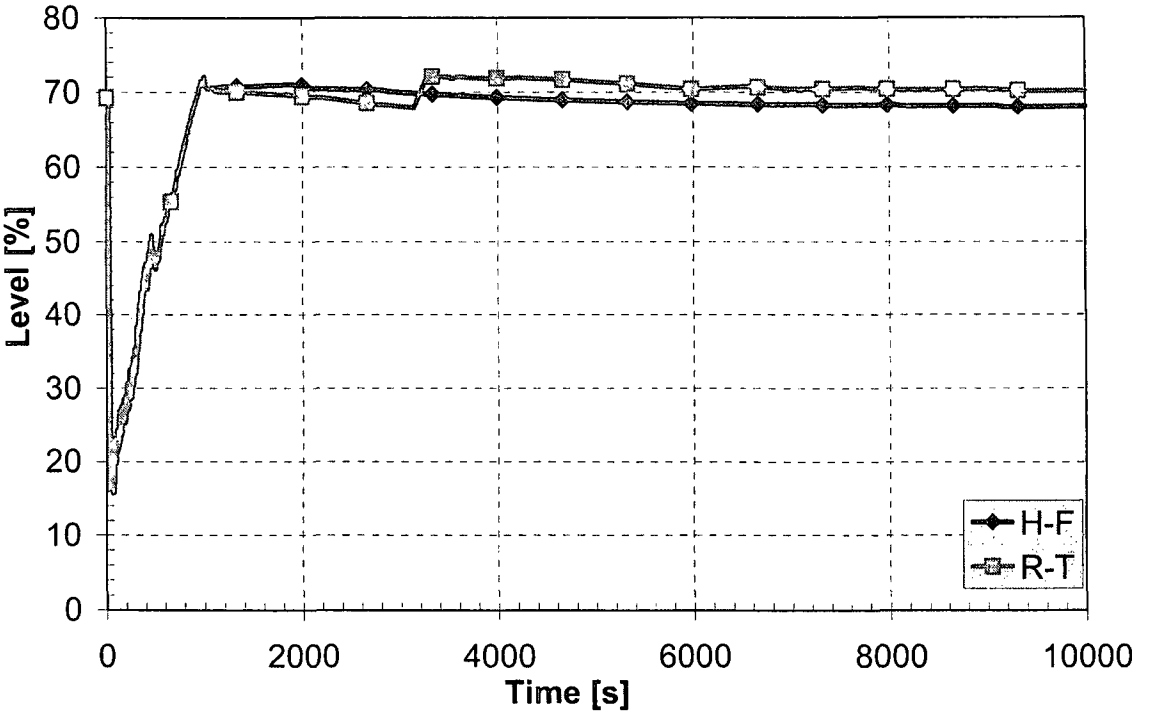

Figure 10 SG 1 level

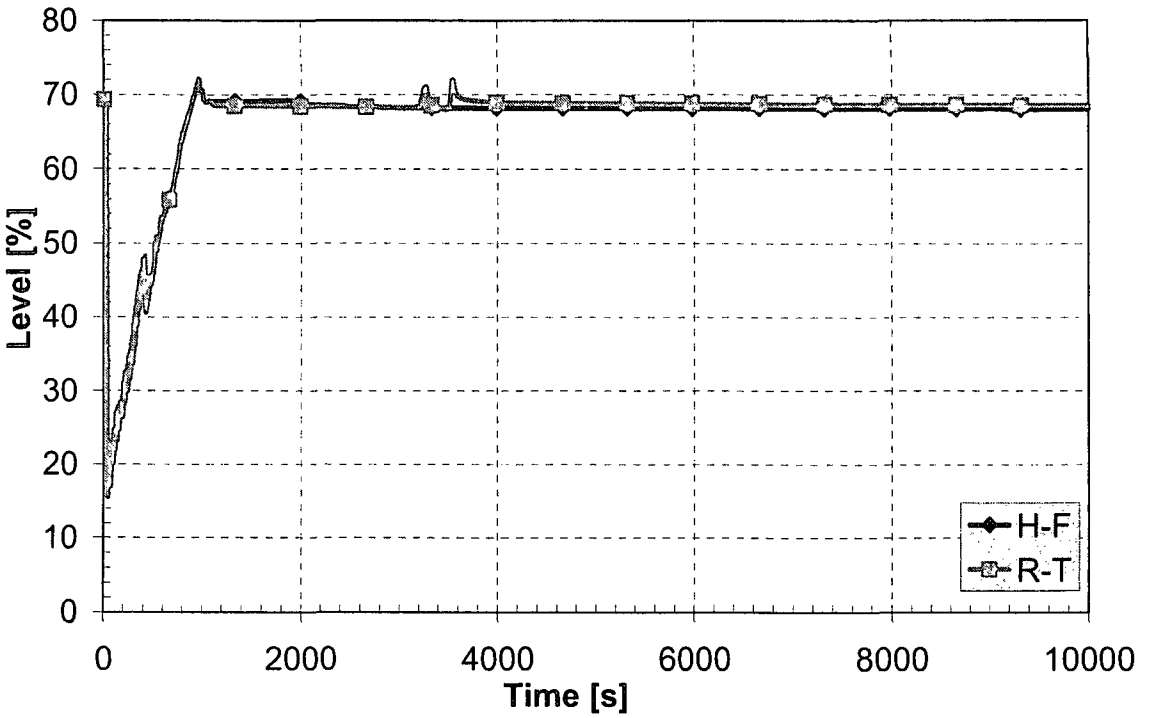

Figure 11 SG 2 level

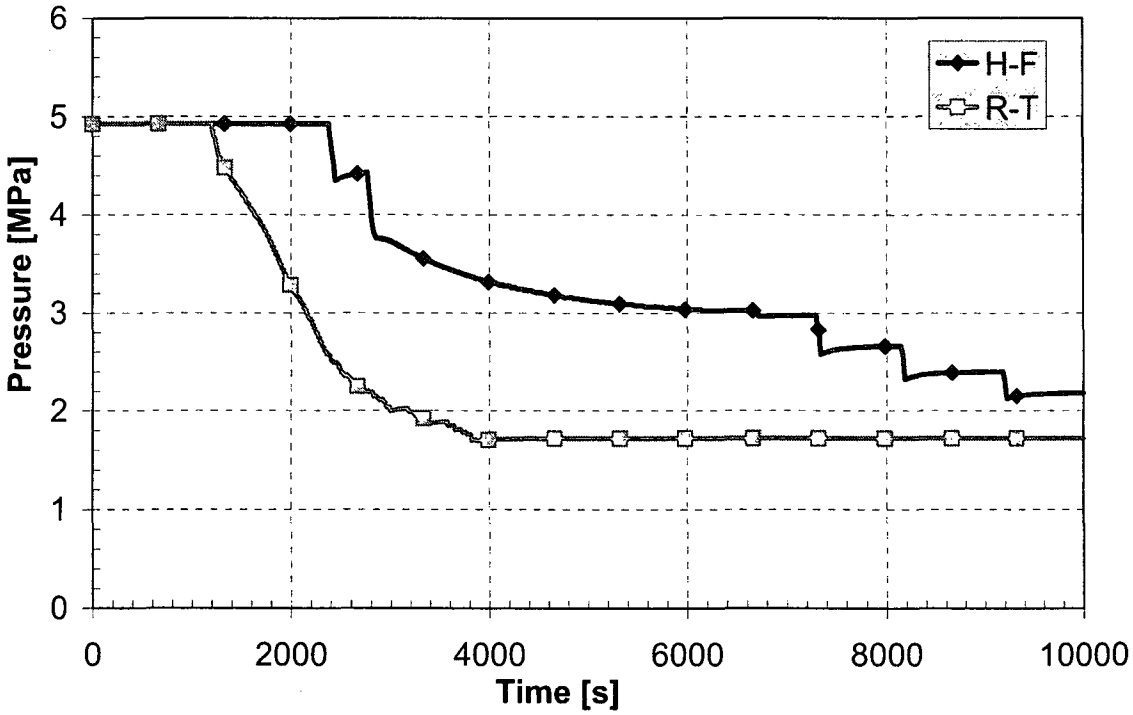

Figure 12 Accumulator No. 1 pressure

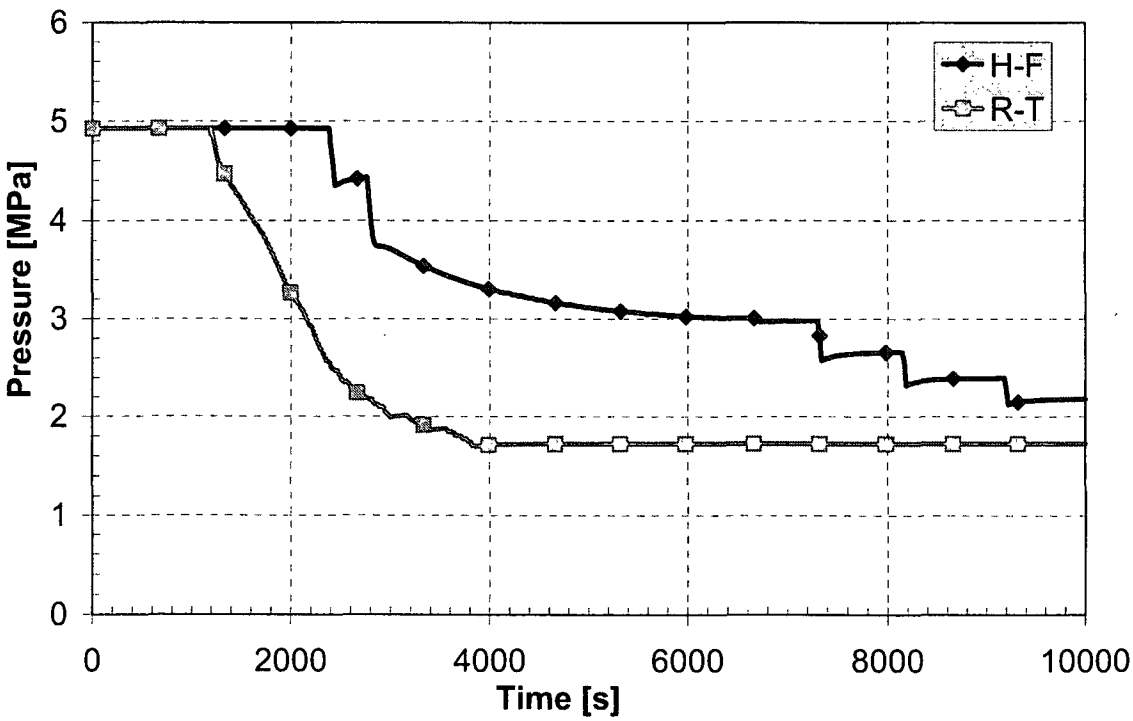

Figure 13 Accumulator No. 2 pressure

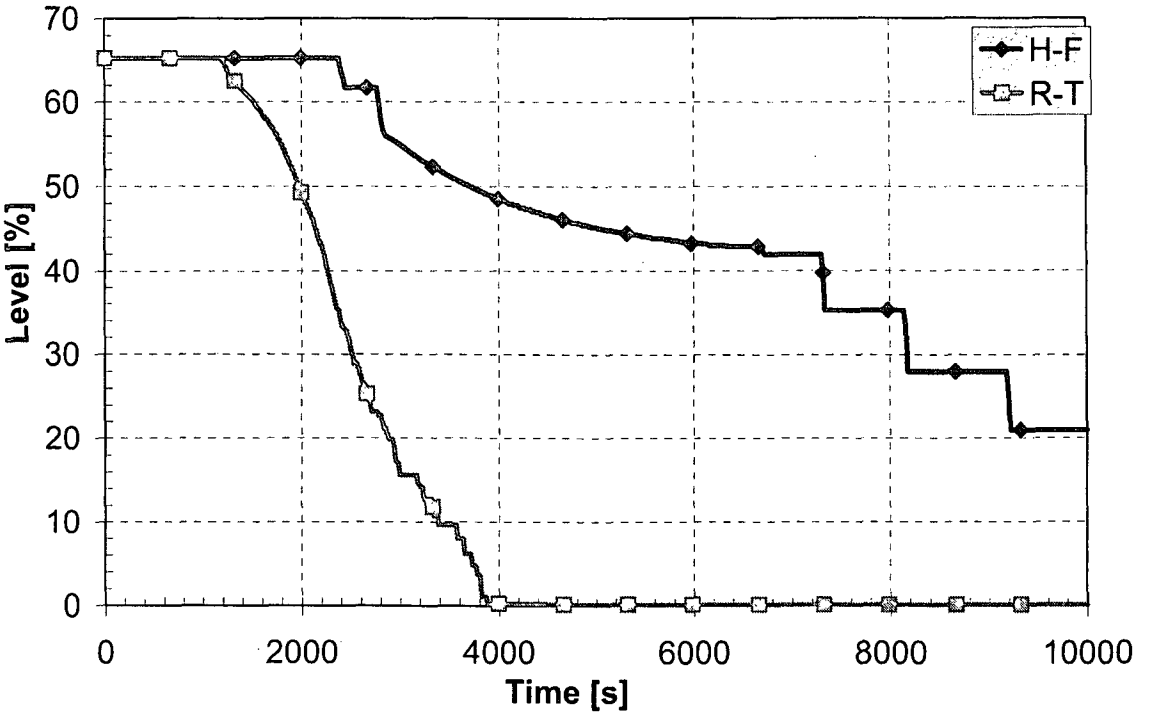

Figure 14 Accumulator No. 1 level

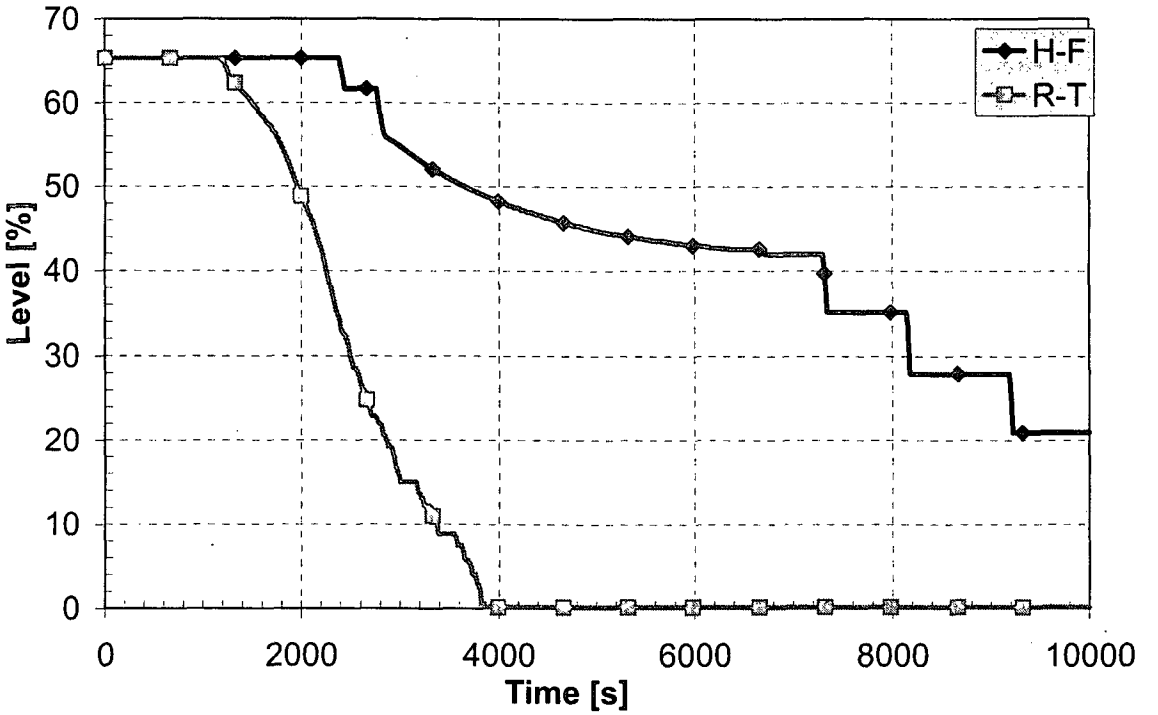

Figure 15 Accumulator No. 2 level

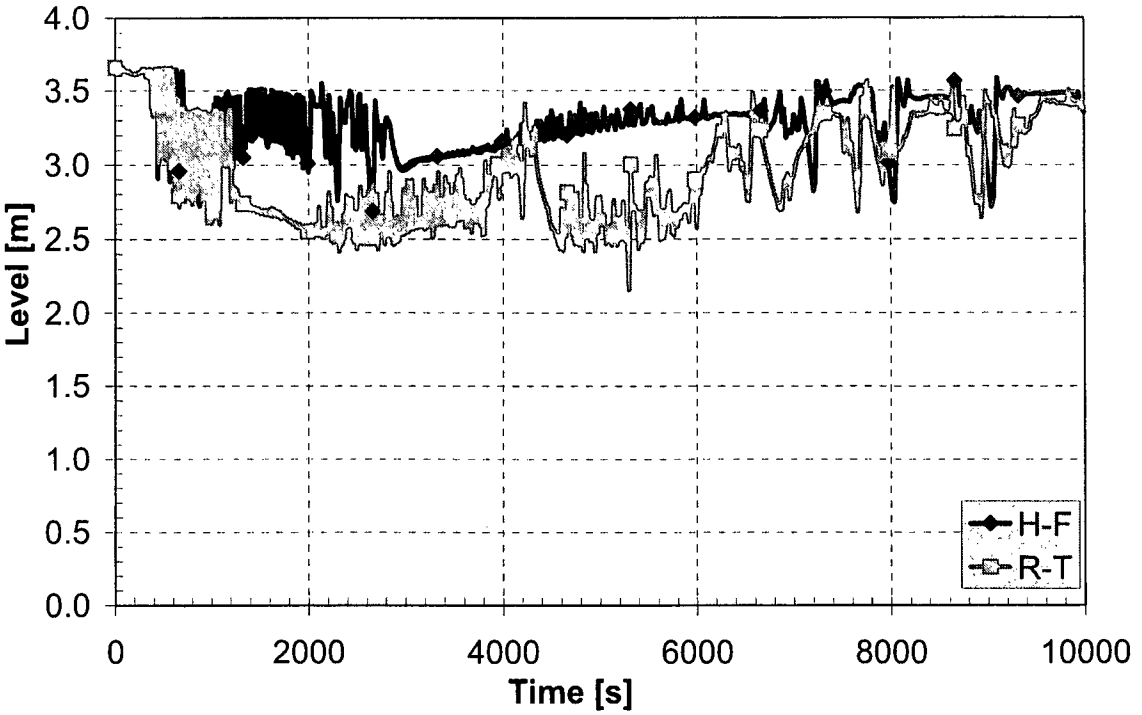

Figure 16 Core collapsed level

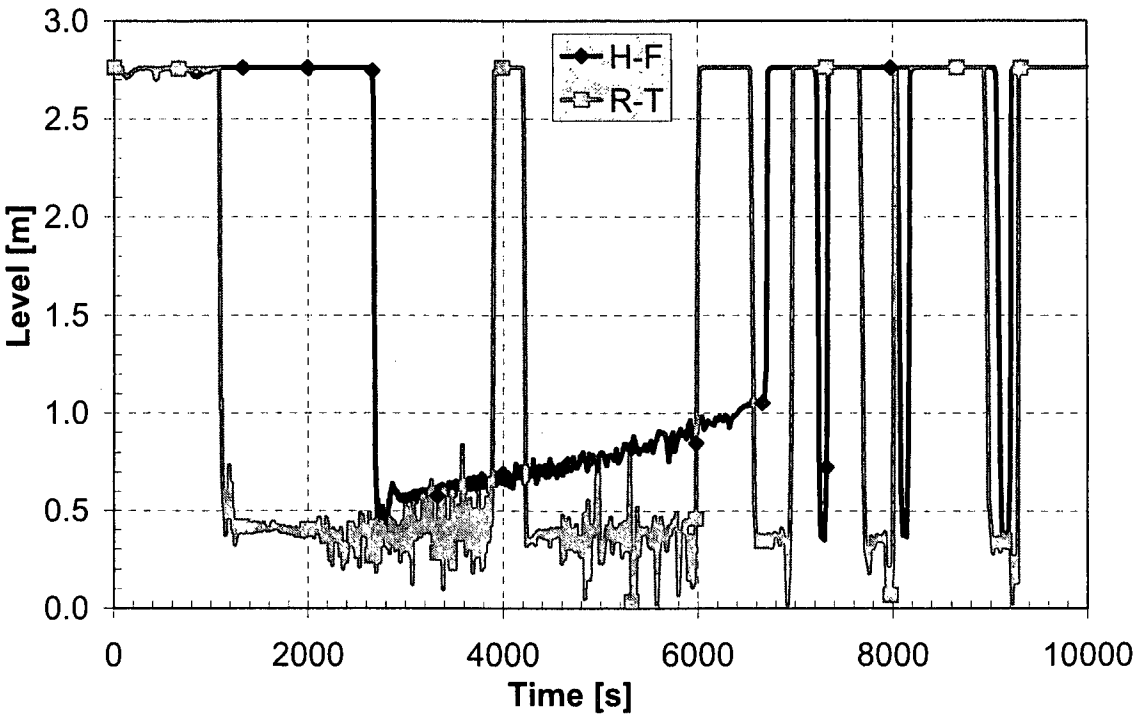

Figure 17 Loop seal No. 1 reactor side collapsed level

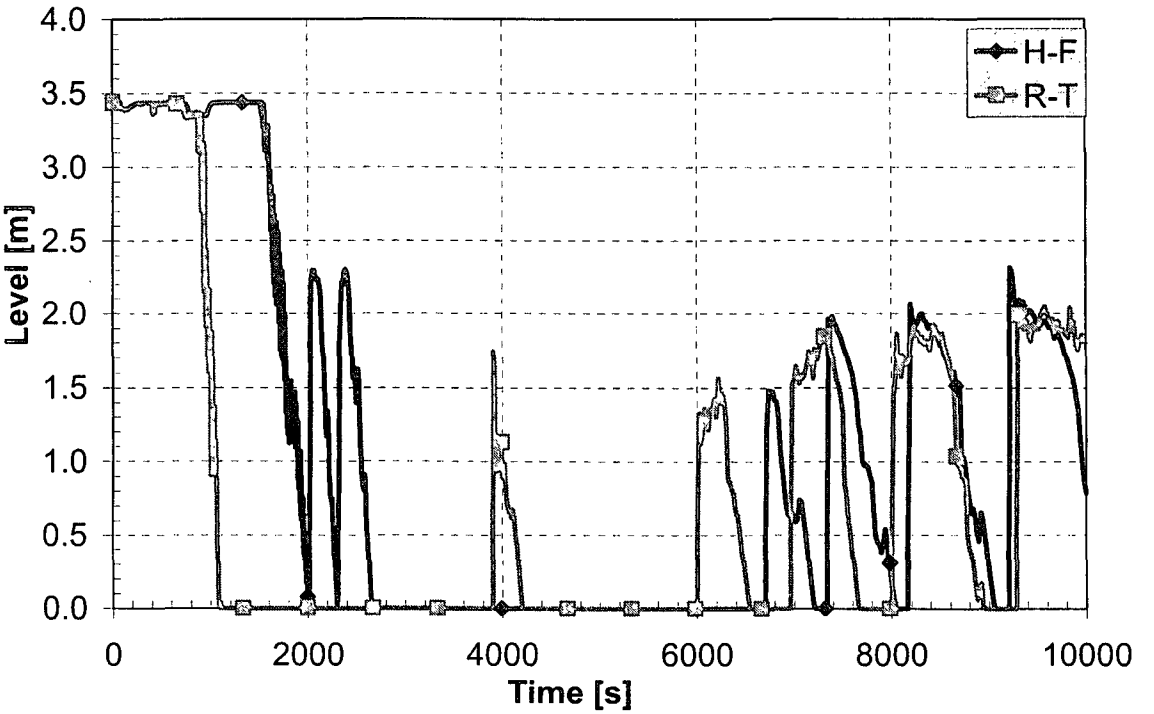

Figure 18 Loop seal No. 1 SG side collapsed level

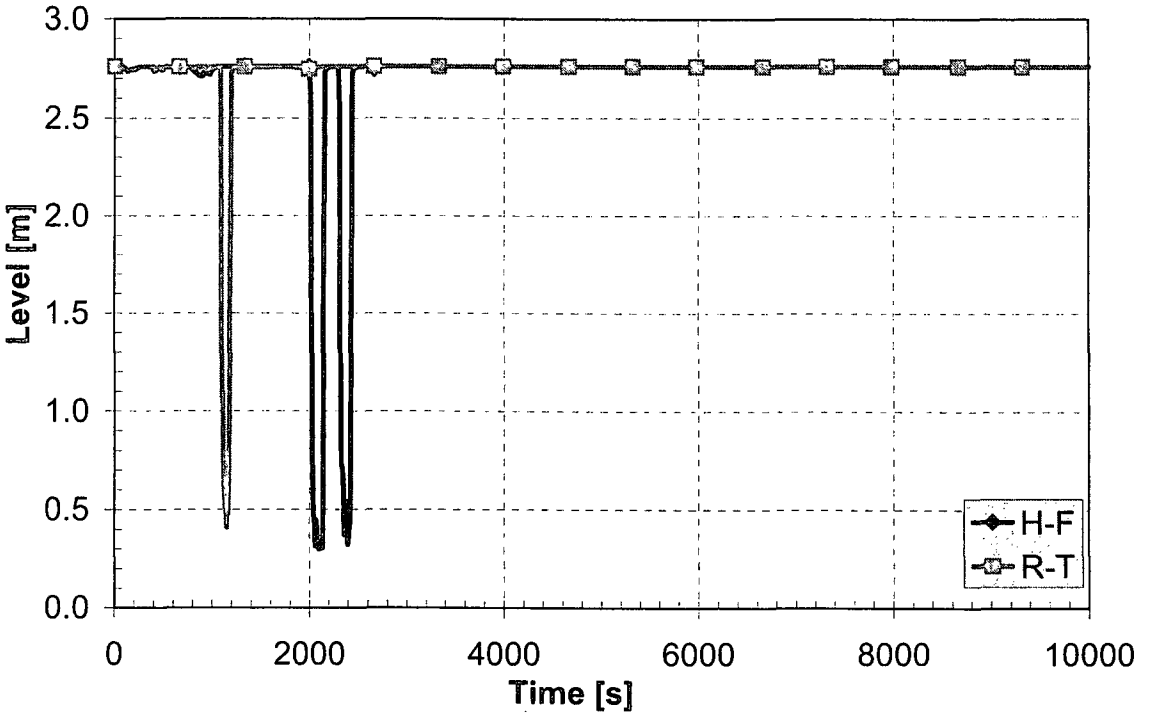

Figure 19 Loop seal No. 2 reactor side collapsed level

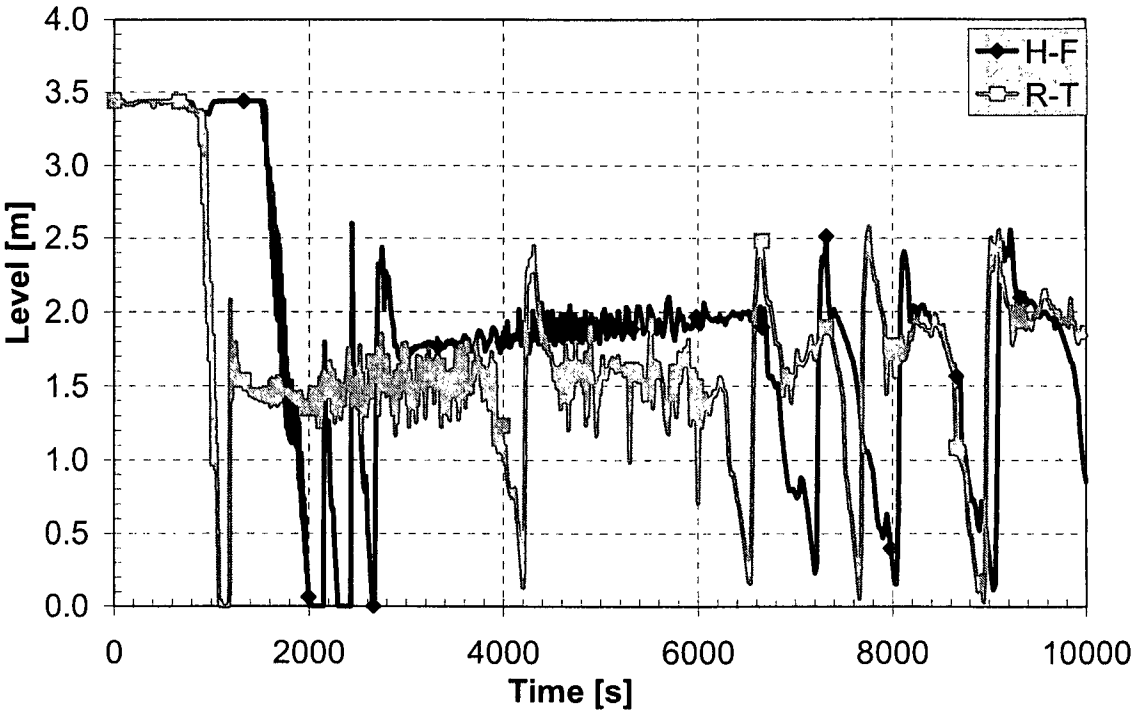

Figure 20 Loop seal No. 2 SG side collapsed level

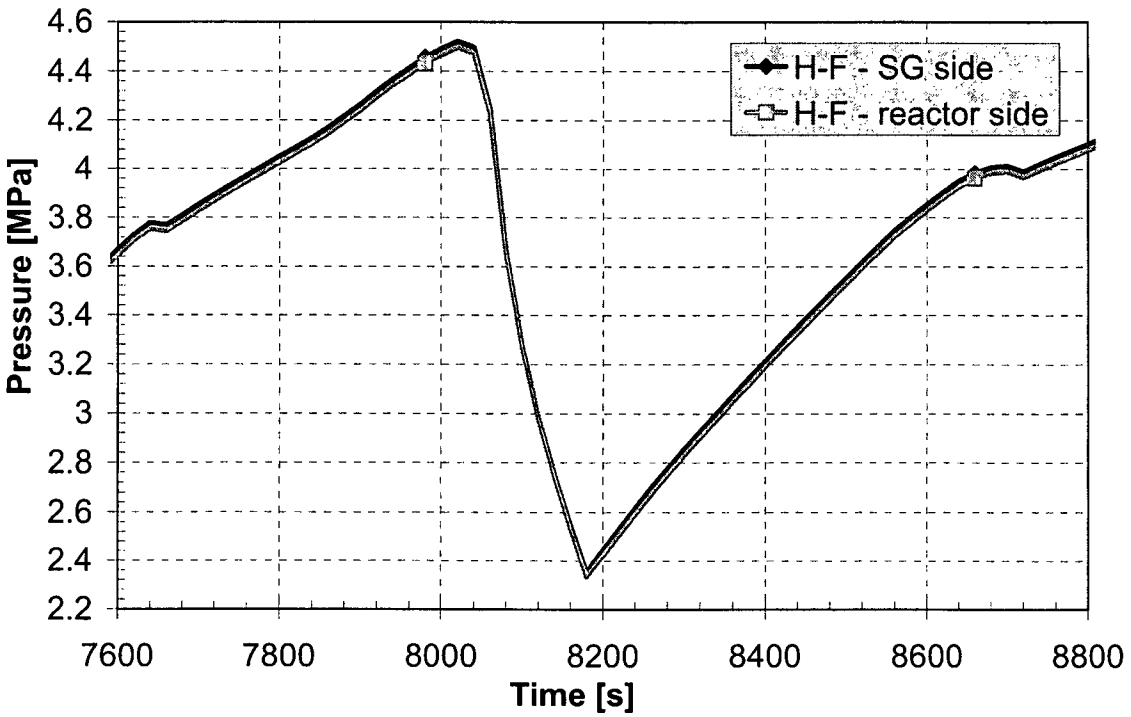

Figure 21 Loop seal No. 1 pressures

5.2 Variation Analyses

Two variation analyses were performed to investigate the vessel bypass configuration and the influence of the offtake model at the break.

5.2.1 Vessel Bypass Configuration Influence

For this analysis, the bypass flow from the reactor vessel downcomer to the upper plenum of the reactor vessel was closed. This assumption is acceptable because temperature changes in the reactor vessel structures can cause some structures to expand more than others, enabling the circular opening between the core barrel and downcomer (where the hot leg loosely enters the core barrel) to reclose (junction 171-02 between downcomer inlet volume 171-01 and upper plenum 125.01).

The other bypass flow was modified at junction 151-01 between upper head volume 151-01 and upper downcomer volume 165-03. For this junction, an additional friction coefficient, FJUNF (and FJUNR), of 10 was introduced.

However, as can be observed from the next set of figures, this change did not significantly influence the transient's course. The case with reduced vessel bypasses is marked "H-F byp.red." on the figures.

The primary pressure (Figure 22) was oscillatory and decreased slightly faster in the H-F byp.red. case than in the default H-F case, which caused HPIS and accumulator injection earlier in the transient. In the first part of the transient, break flow was similar on average to the default H-F case, but somewhat smoother. In the later phase of the transient, more oscillatory break flow can be observed in the H-F byp.red. case, which is slightly higher on average than in the H-F case (Figure 23). As a result, primary mass depletion was no deeper; however, more oscillatory behavior can be observed in the H-F byp.red. case (Figure 24).

Some differences can be seen in the core collapsed level, which, because of the slightly larger break flow, stayed at a slightly lower level than in the H-F case, although it was more oscillatory (Figure 25). The loop seal levels (Figures 26, 27, 28, and 29) also reflect these oscillations.

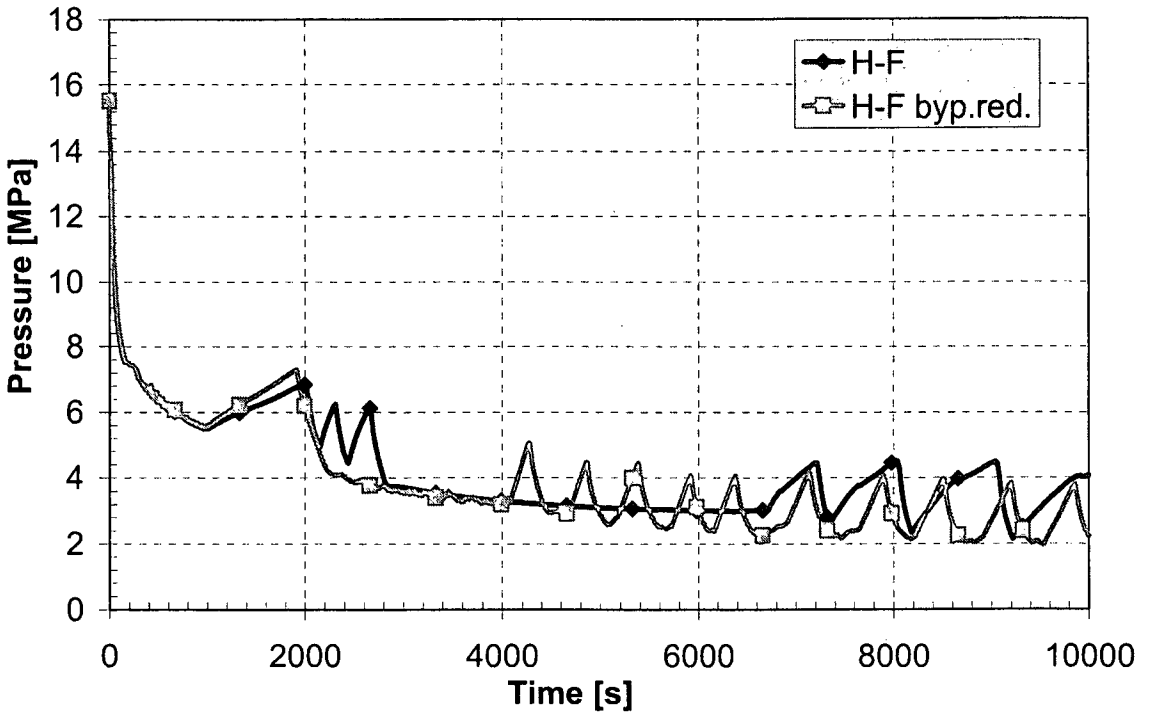

Figure 22 Primary pressure—vessel bypass variation

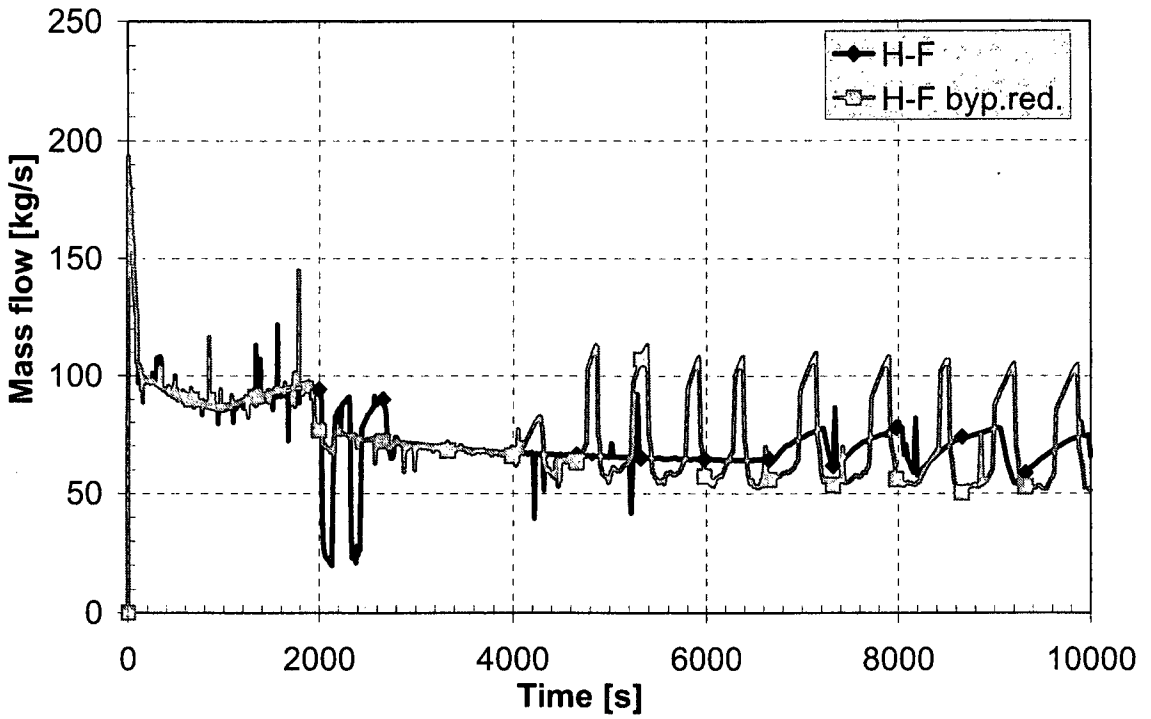

Figure 23 Break flow—vessel bypass variation

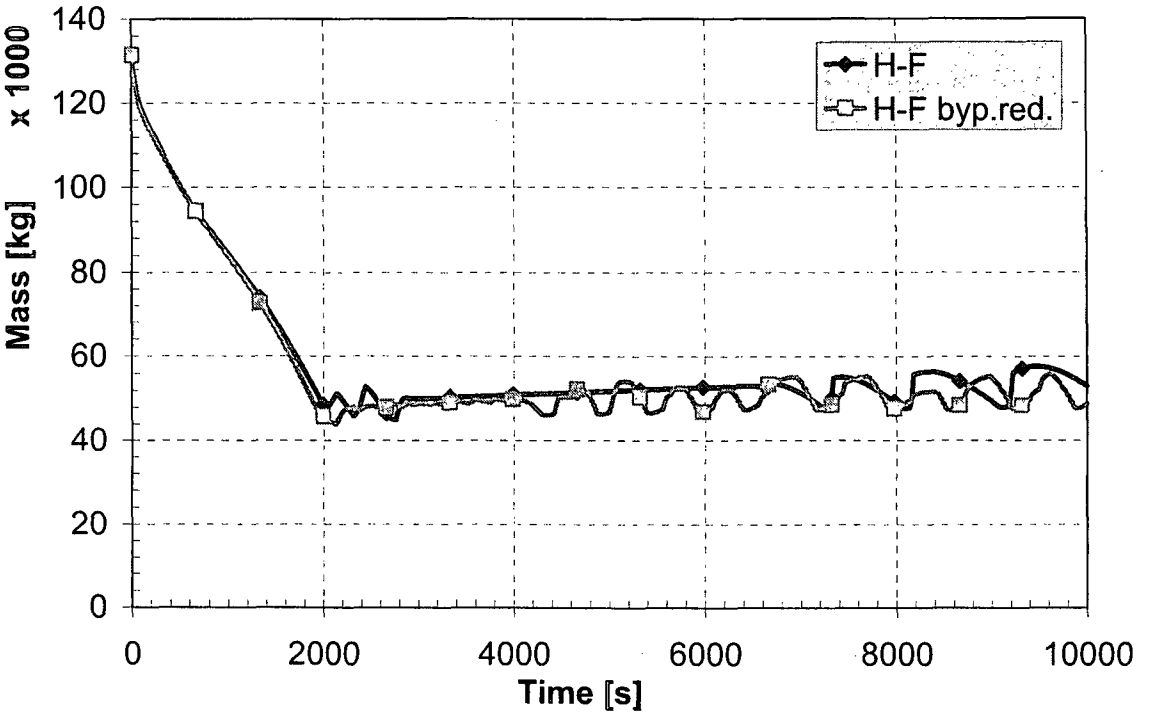

Figure 24 Primary mass—vessel bypass variation

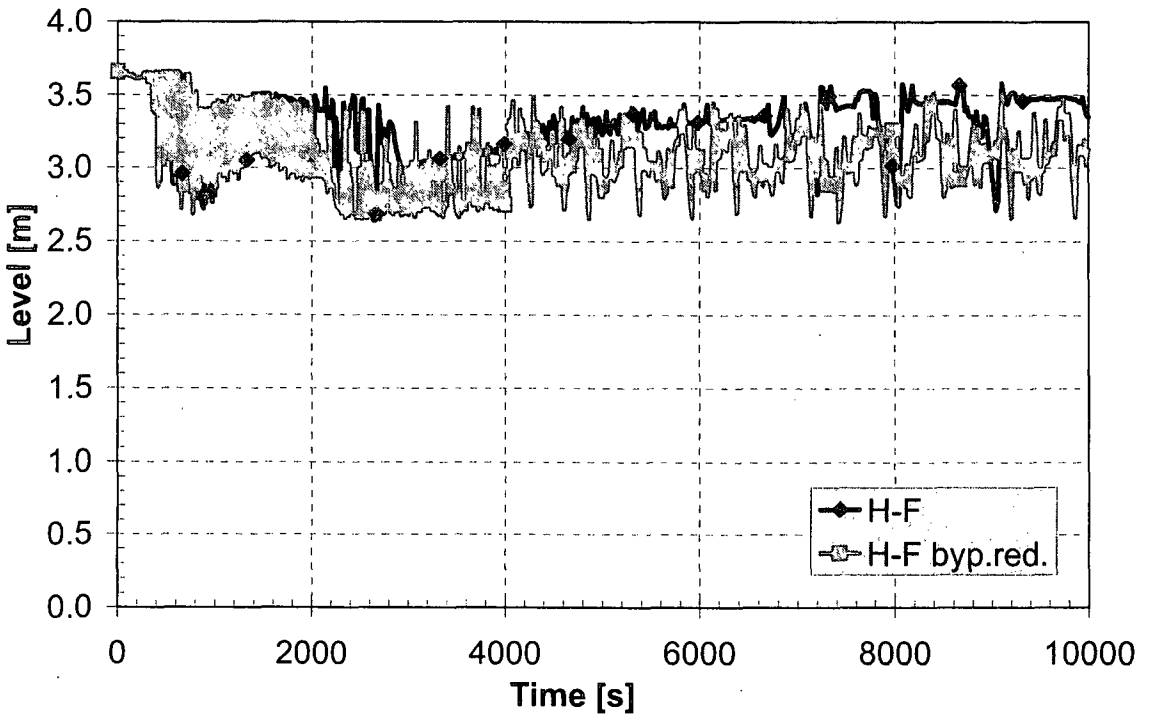

Figure 25 Core collapsed level—vessel bypass variation

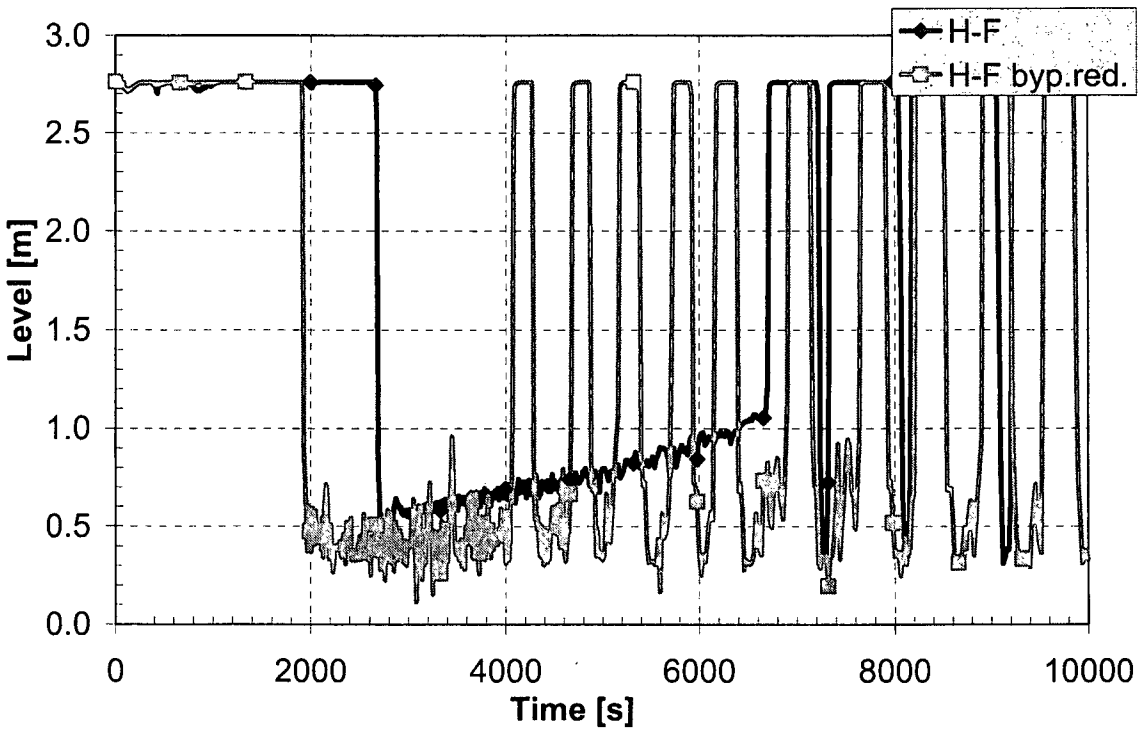

Figure 26 Loop seal No. 1 reactor side collapsed level—vessel bypass variation

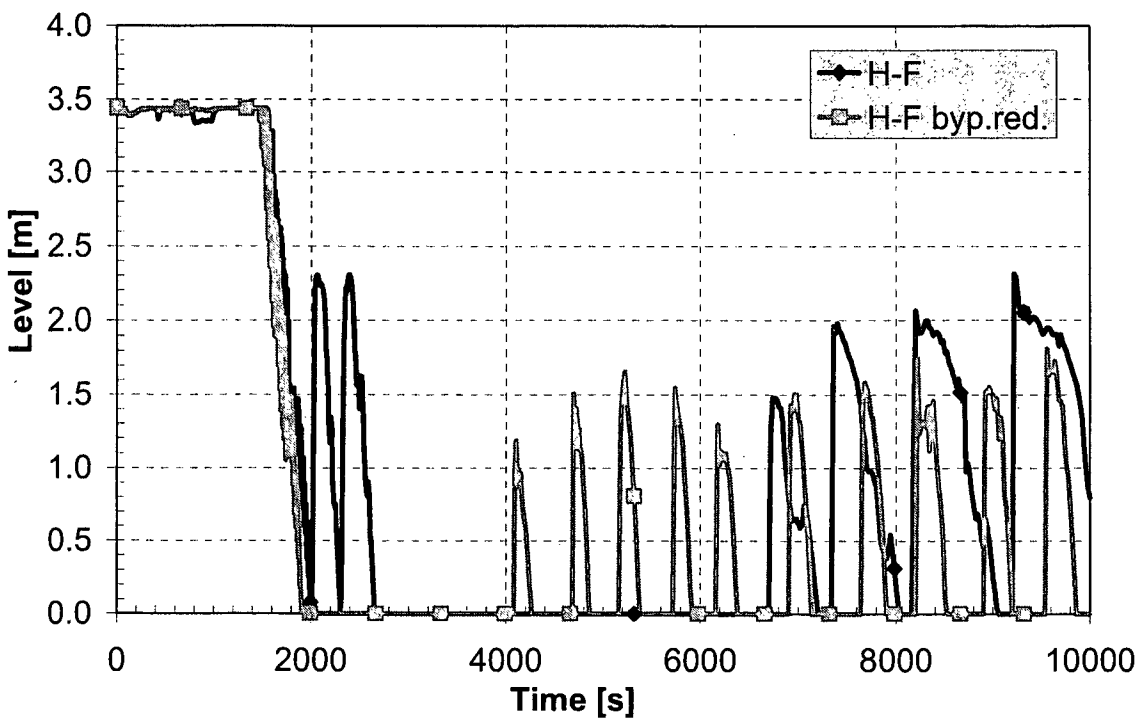

Figure 27 Loop seal No. 1 SG side collapsed level—vessel bypass variation

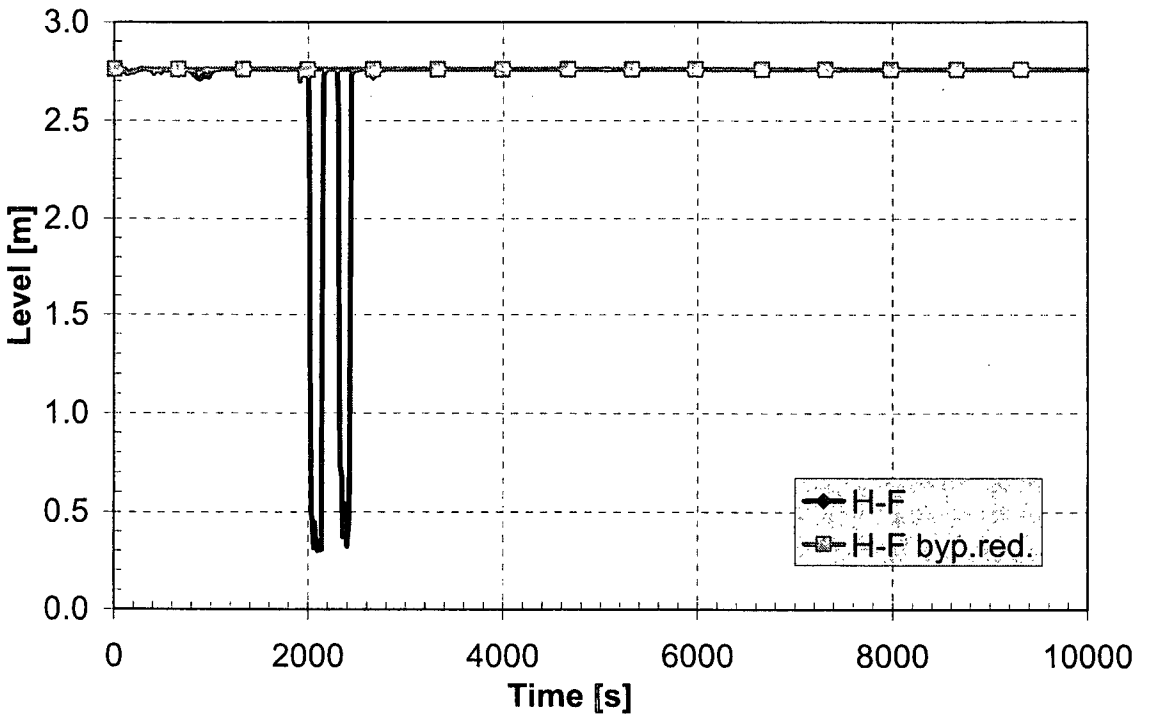

Figure 28 Loop seal No. 2 reactor side collapsed level—vessel bypass variation

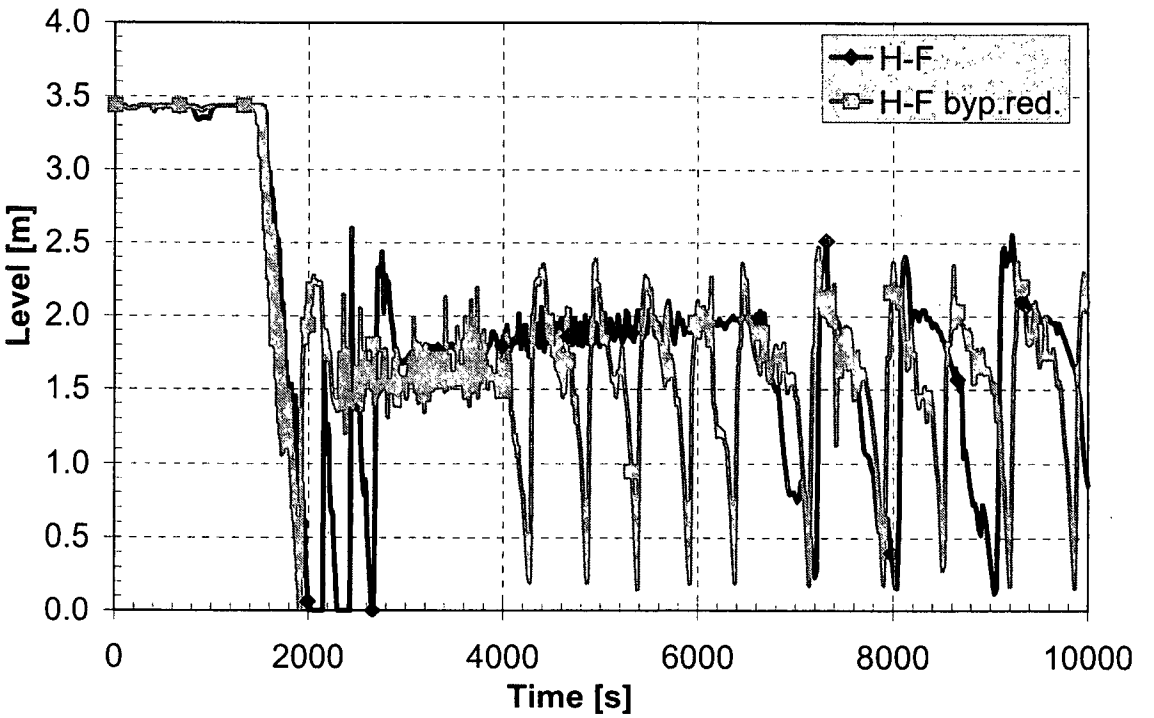

Figure 29 Loop seal No. 2 SG side collapsed level—vessel bypass variation

5.2.2 Offtake Model Influence

The next set of figures includes the offtake model, marked as "H-F offtake," at the break and shows a similar, although smaller, effect to the previous variation in reactor vessel bypass configuration. Specifically, the enlarged insurge of vapor through the liquid phase into the break enabled a slightly faster primary pressure decrease (Figure 30) in the later phase of the transient.

The offtake model reflected a slightly lower void fraction in the vicinity of the break (Figure 31), since it was transported faster through the break (Figure 32). This had a smaller influence on the loop seal clearing process (Figure 33) and an even smaller influence on the core collapsed level development (Figures 34 and 35).

However, many calculation problems appeared in the vicinity of the break during the accumulator discharge period. These problems may have been the consequence of cold water flowing into the cold leg, which caused additional problems in calculating water properties in volume 375-01. The time step was reduced by a factor of 10, which produced significantly larger consumption of CPU time. In addition, the code aborted on several occasions; thus, after several restarts with the reduced time step, the calculation was finally interrupted before 5,000 seconds of transient time.

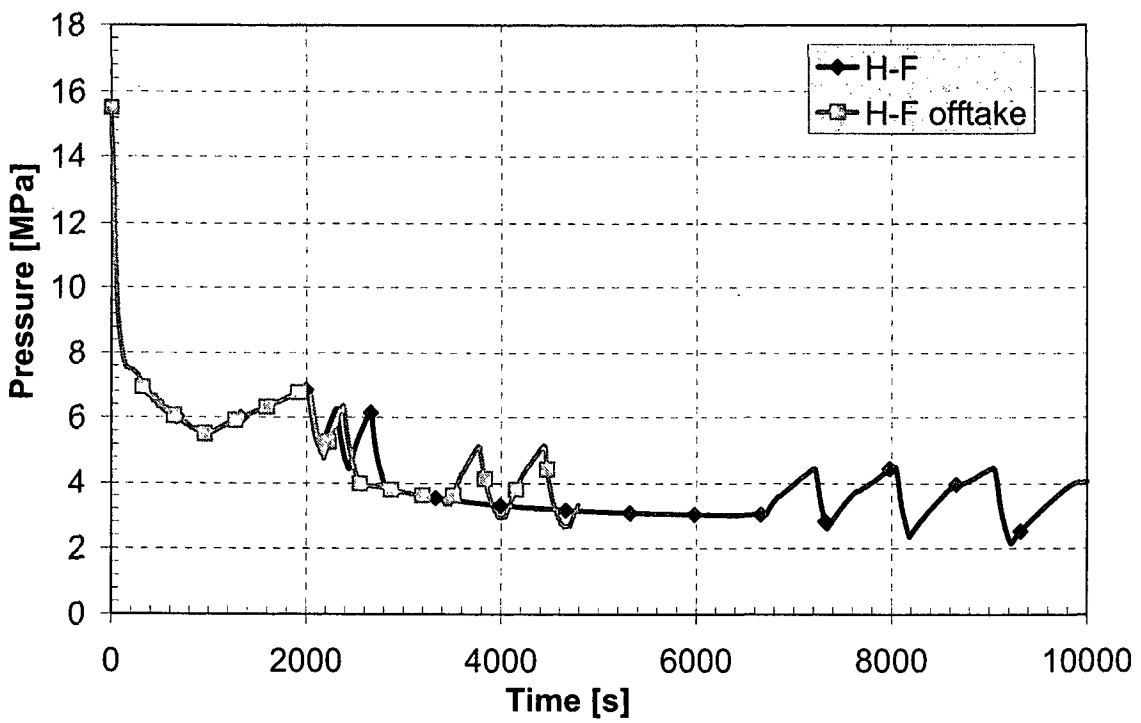

Figure 30 Primary pressure—offtake model

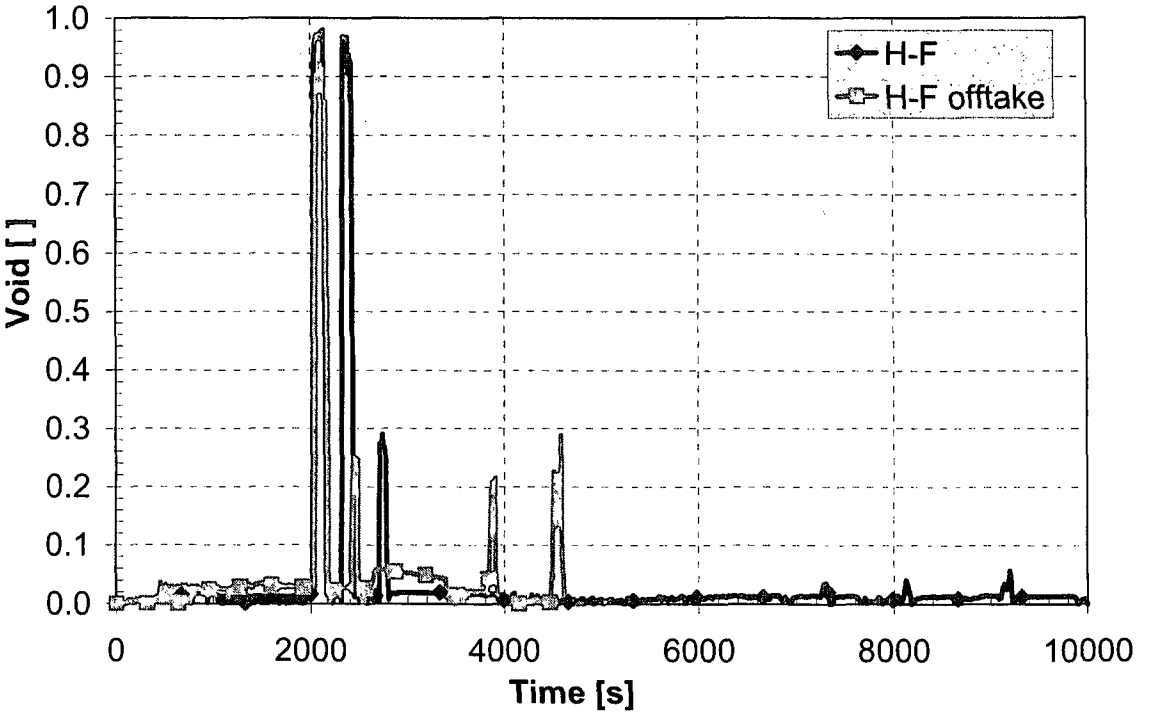

Figure 31 Void fraction at the break—offtake model

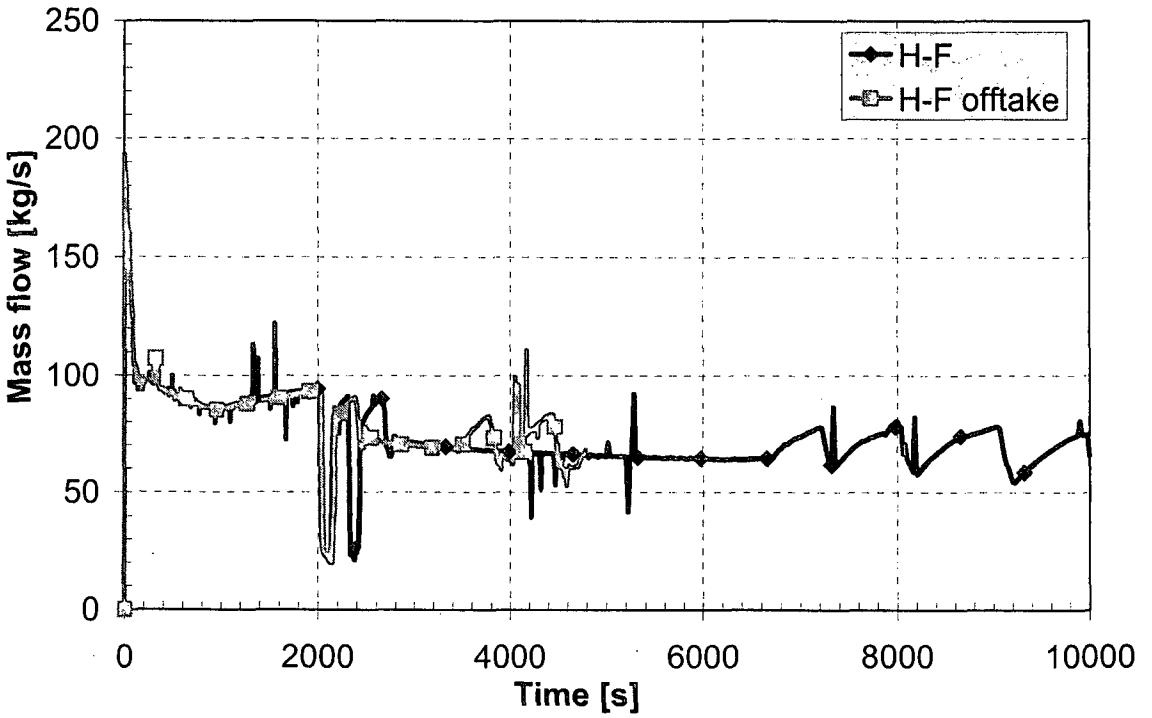

Figure 32 Break flow—offtake model

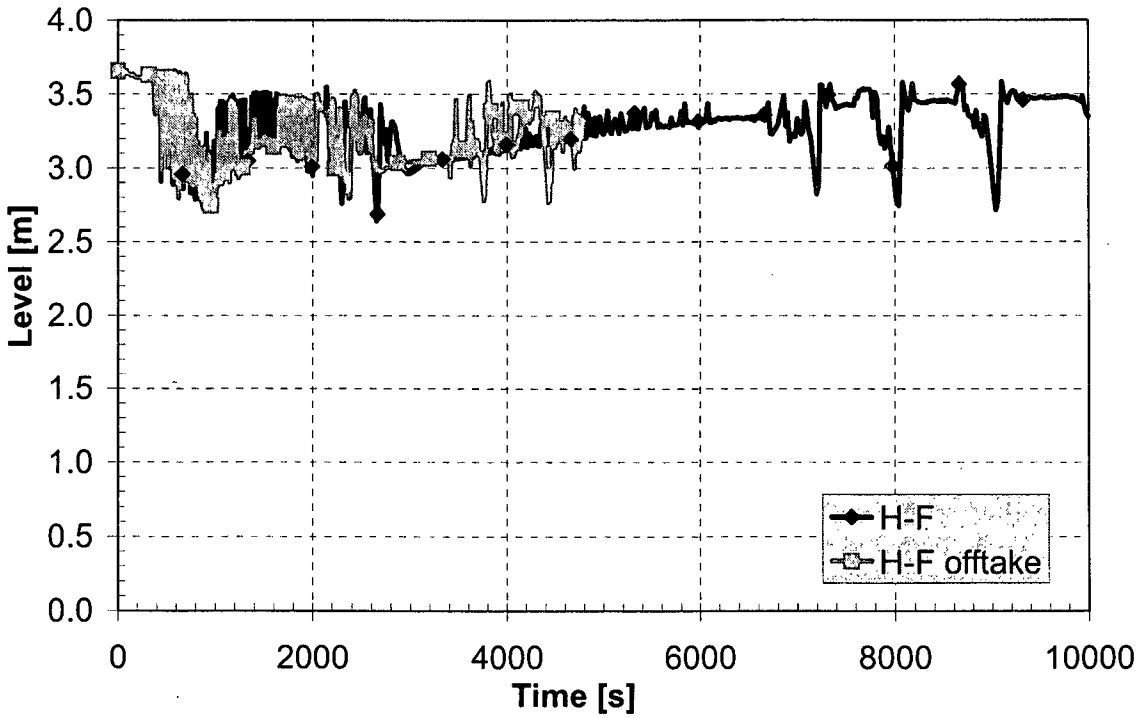

Figure 33 Core collapsed level—offtake model

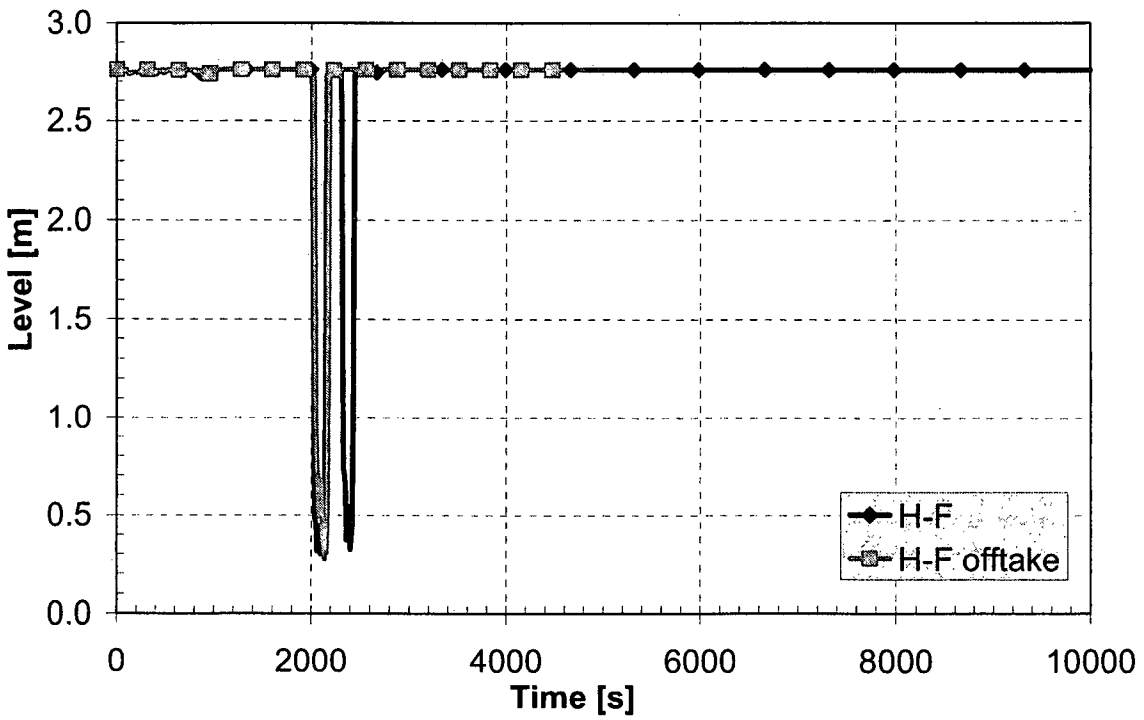

Figure 34 Loop seal No. 2 reactor side collapsed level—offtake model

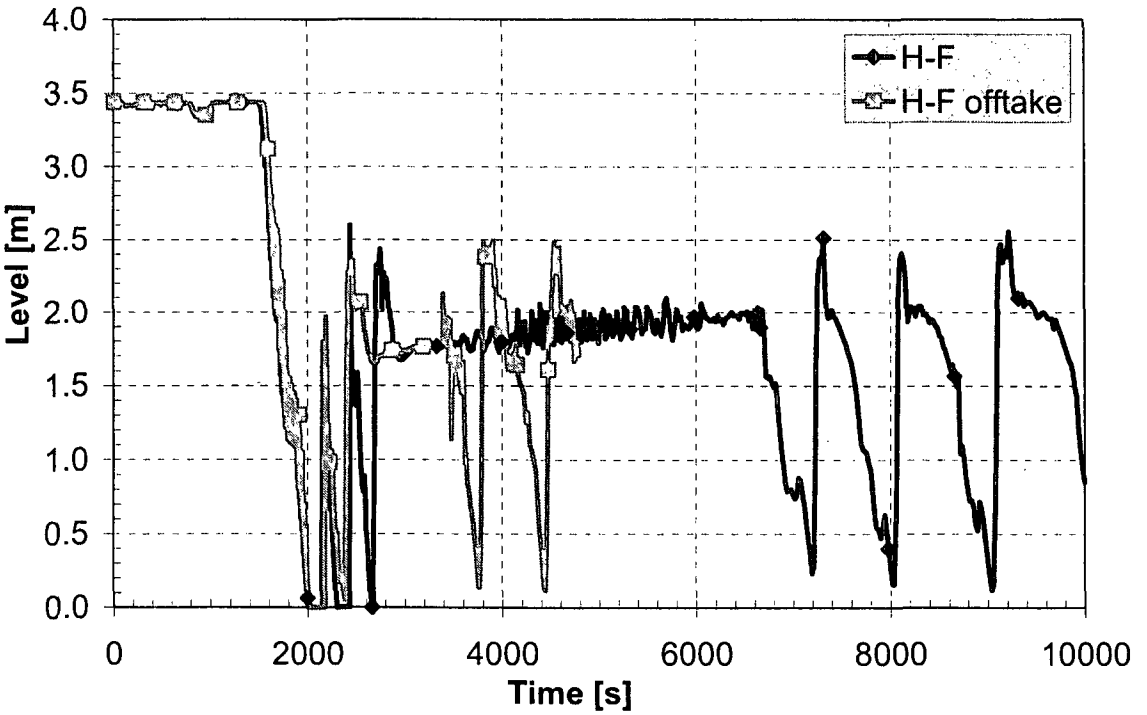

Figure 35 Loop seal No. 2 SG side collapsed level—offtake model

6. RELAP5/MOD3.3 RUN STATISTICS

MOD3.3 calculations were performed on a SUN FIRE V880 server with four UltraSPARC III 750-megahertz processors and 16 gigabytes of main RAM, running under the SOLARIS 9 operating system.

Table 1 shows run-time statistics for the two analyzed base cases, H-F and R-T.

Table 1 Run-Time Statistics

Analyzed case	Computer CPU time (s)	Total number of time steps (NT)	Total number of volumes (N)	Grind time CPU/(NT*N)
both cases — 1000 s of steady state	3516.21	26303	469	2.85E-04
Henry-Fauske (H-F) — default	38525.94	292310	469	2.81E-04
Ransom-Trapp (R-T)	49307.04	373392	469	2.82E-04

Figure 36 illustrates the CPU time consumed for the two base analyses cases (H-F and R-T).

Figures 37 to 39, respectively, show the mass error, time step, and Courant Δt for the two base analyses cases (H-F and R-T).

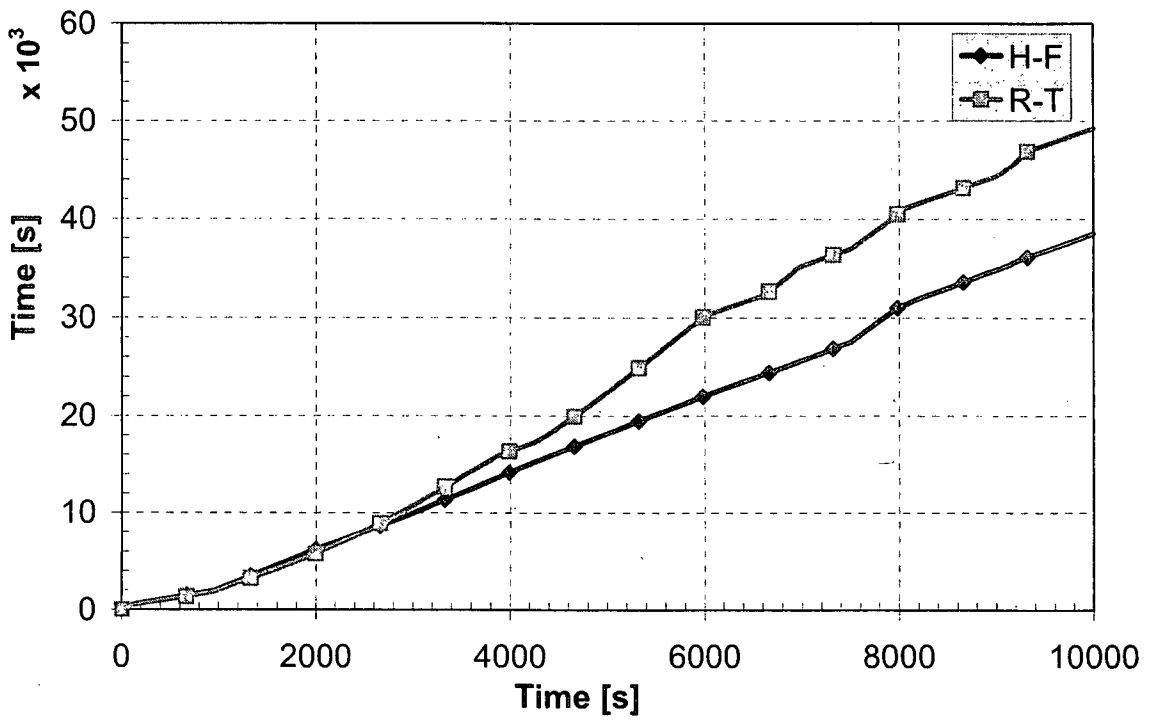

Figure 36 CPU time consumed for two base analyses cases (H-F and R-T)

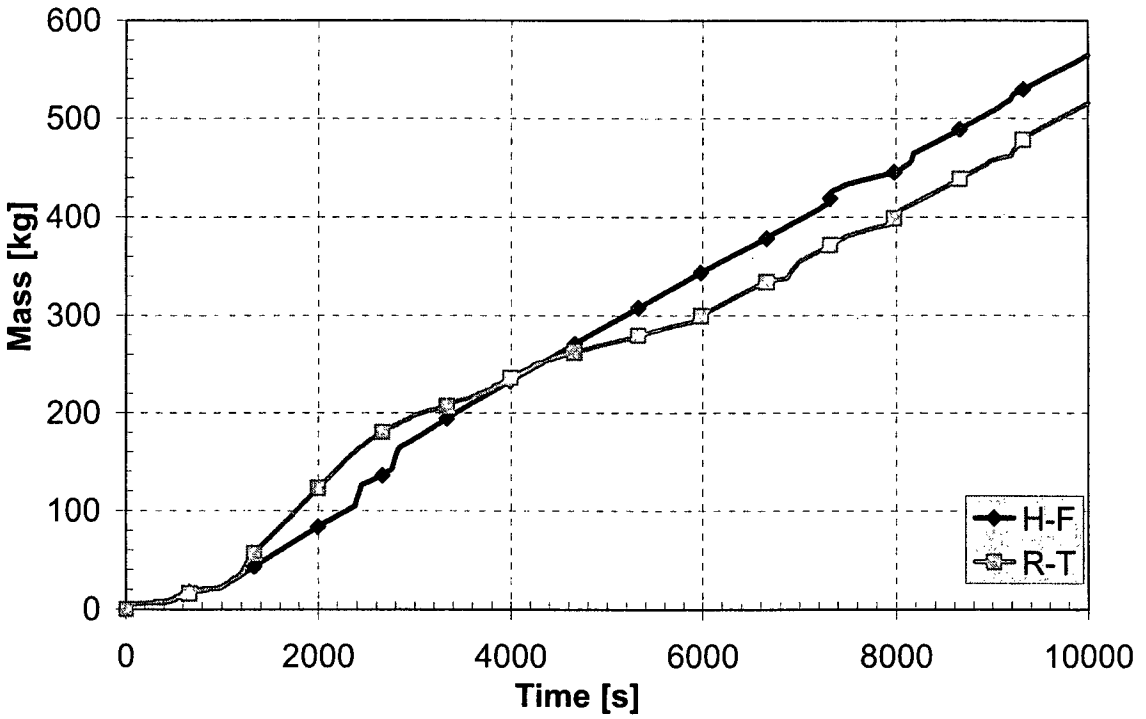

Figure 37 Mass error for two base analyses cases (H-F and R-T)

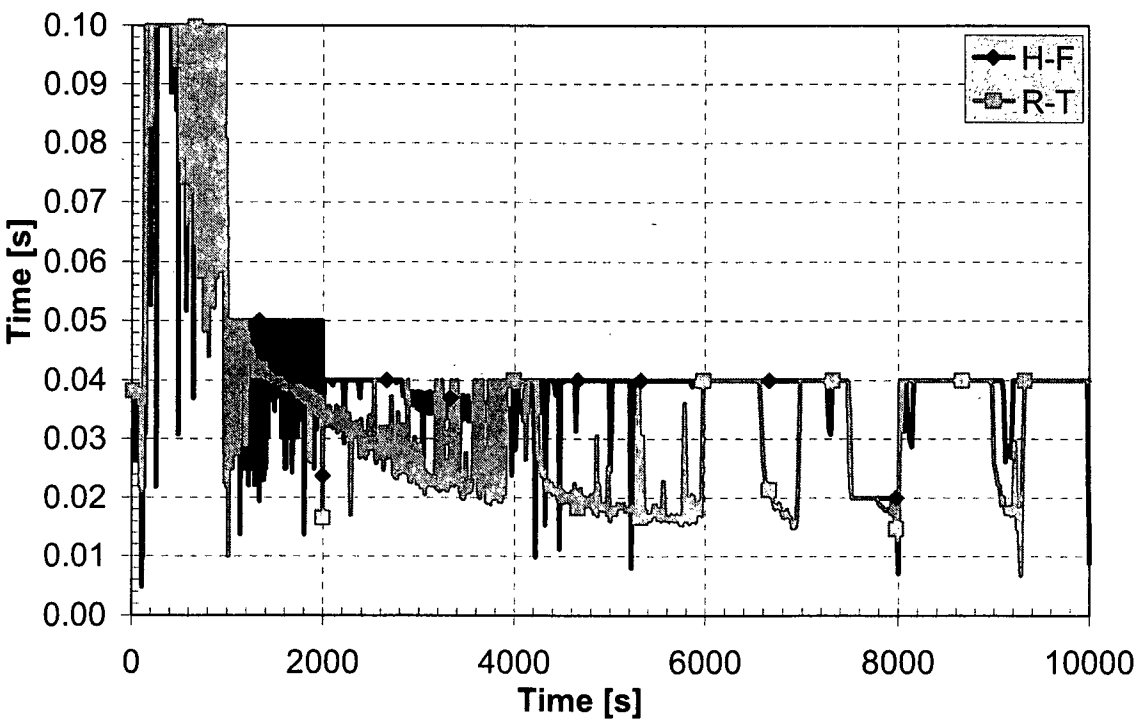

Figure 38 Time step for two base analyses cases (H-F and R-T)

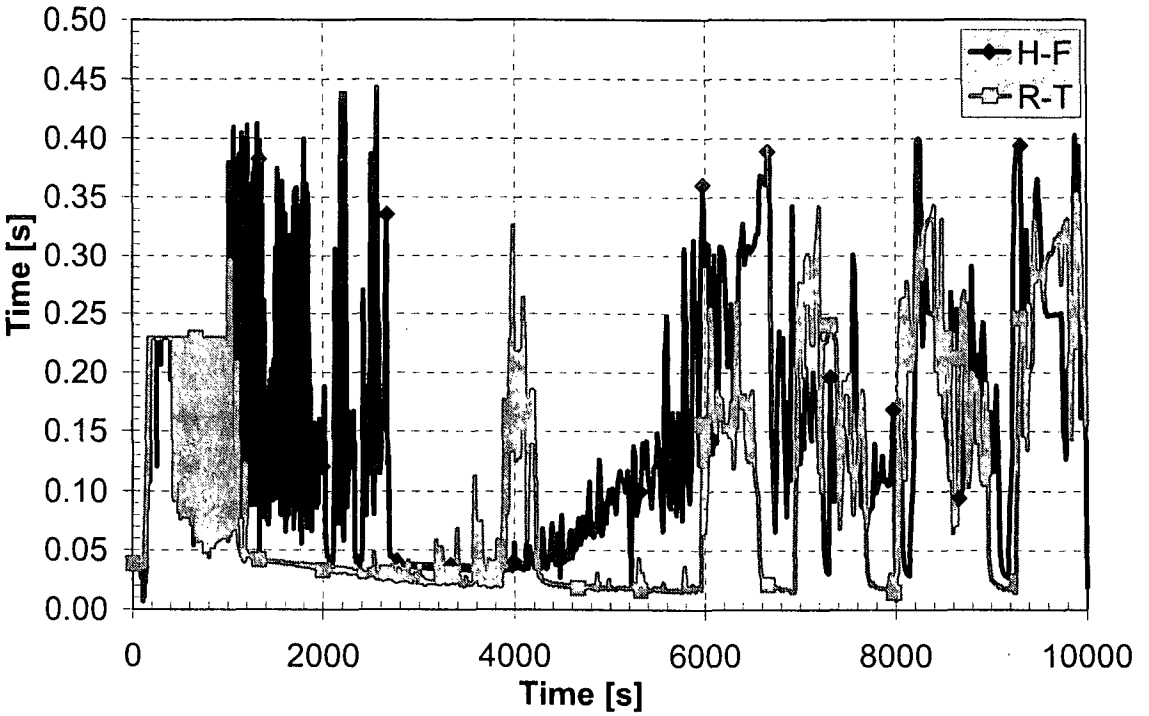

Figure 39 Courant Δt for two base analyses cases (H-F and R-T)

7. CONCLUSIONS

The 2-inch LOCA transient was analyzed for Krško NPP using the KFSS for verification. The results indicated standard LOCA behavior with fast initial primary pressure decrease and loop seal clearing phenomena.

The ECCS mitigated the consequences of the LOCA accident initiated by the break in cold leg No. 2 between the RCP and reactor vessel.

In the later phase of the transient, somewhat oscillatory behavior of the various parameters was observed, which caused multiple loop seal clearing cycles. This was found to be the consequence of the periodic flooding of both loop seals by the cold borated water from the HPIS, accumulators, and LPIS.

The mechanism of loop seal clearing phenomena was investigated for this specific case. It was shown that large pressure spikes originate in ECCS behavior and do not represent nonphysical results.

Using some variation cases, the influence of the vessel bypass configuration and the offtake model at the break location was also studied. The results showed that these two model variations do not significantly affect the transient course.

The ECCS model should be improved, since the HPIS and LPIS pumps are modeled as time-dependent junctions, although their flow depends on filtered primary pressure to smooth the time-dependent junction response.

8. REFERENCES

1. American National Standards Institute/American Nuclear Society, "Nuclear Power Plant Simulators for Use in Operator Training and Examination (Revision of ANSI/ANS-3.5-1993 and ANSI/ANS-3.5-1985)," ANSI/ANS-3.5-1998.

2. I. Parzer and A. Prošek, SB LOCA thermal-hydraulic analysis for Krško full scope simulator validation, Proceedings of International Conference Nuclear Energy for New Europe 2005, September 5-8, 2005, Bled, Slovenia. Proceedings. Ljubljana: Nuclear Society of Slovenia, 2005, pp. 015-1-015-9.

3. U.S. Nuclear Regulatory Commission, "RELAP5/MOD3.3 Code Manual," Vol. 1, "Code Structure, System Models, and Solution Methods"; Vol. 2, "Users' Guide and Input Requirements"; Vol. 3, "Developmental Assessment Problems"; Vol. 4, "Models and Correlations"; Vol. 5, "Users' Guidelines"; Vol. 6, "RELAP5/MOD3 Code Manual—Validation of Numerical Techniques in RELAP5/MOD3.0"; Vol. 7, "Summaries and Reviews of Independent Code Assessment Reports"; and Vol. 8, "Programmers Manual," NUREG/CR_5535, Rev. 1, December 2001.

4. V. H. Ransom and J. A. Trapp. "The RELAP5 Choked Flow Model and Application to a Large Scale Flow Test." Proceedings of the ANS/ASME/NRC International Topical Meeting on Nuclear Reactor Thermal-Hydraulics, Saratoga Springs, New York, October 5-8, 1980, pp. 799-819.

NRC FORM 335 (9-2004) NRCMD 3.7

U.S. NUCLEAR REGULATORY COMMISSION

BIBLIOGRAPHIC DATA SHEET

(See instructions on the reverse)

1. REPORT NUMBER (Assigned by NRC, Add Vol., Supp., Rev., and Addendum Numbers, If any.)
NUREG/IA-0222

2. TITLE AND SUBTITLE
Analysis of RELAP5/MOD3.3 Prediction of 2-Inch Loss-of-Coolant Accident at Krško Nuclear Power Plant

3. DATE REPORT PUBLISHED
MONTH: March
YEAR: 2010

4. FIN OR GRANT NUMBER

5. AUTHOR(S)
Iztok Parzer, Borut Mavko

6. TYPE OF REPORT
Technical

7. PERIOD COVERED *(Inclusive Dates)*

8. PERFORMING ORGANIZATION - NAME AND ADDRESS *(If NRC, provide Division, Office or Region, U.S. Nuclear Regulatory Commission, and mailing address; if contractor, provide name and mailing address.)*

Jožef Stefan Institute
Jamova cesta 39
SI-1000 Ljubljana, Slovenia

9. SPONSORING ORGANIZATION - NAME AND ADDRESS *(If NRC, type "Same as above"; if contractor, provide NRC Division, Office or Region, U.S. Nuclear Regulatory Commission, and mailing address.)*
Division of Systems Analysis
Office of Nuclear Regulatory Research
U.S. Nuclear Regulatory Commission
Washington, DC 20555-0001

10. SUPPLEMENTARY NOTES
A. Calvo, NRC Project Manager

11. ABSTRACT *(200 words or less)*

The purpose of this analysis was to perform calculations of the loss-of-coolant accident (LOCA) for simulator verification and validation and to study the thermal-hydraulic response of the reactor coolant system.

For the thermal-hydraulic analysis, the RELAP5/MOD3.3 code and input model provided by Krško Nuclear Power Plant was used. A small-break LOCA scenario was analyzed to estimate plant response to the opening of a break in cold leg No. 2 between the reactor coolant pump and the reactor pressure vessel. For the purpose of the analysis, the equivalent diameter of the cross-sectional area of the break was set to 5.08 centimeters (2 inches).

In the presented study, the 2-inch LOCA scenario for the Krško Nuclear Power Plant was analyzed with regard to the differences between the Henry-Fauske and the Ransom-Trapp critical flow model. In addition, the study investigated the effect of the special offtake flow model at the break. Some variation cases were also run to capture the effect of flow bypasses in the reactor vessel on the loop seal clearing phenomena.

12. KEY WORDS/DESCRIPTORS *(List words or phrases that will assist researchers in locating the report.)*
Loss-of-coolant accident (LOCA)
Thermalhydraulic code calculations
RELAP5/MOD3.3
Krško NPP
Henry-Fauske
Ransom-Trapp
Westinghouse two-loop pressurized-water reactor (PWR) plant
Jožef Stefan Institute
Republic of Slovenia
Nuclear steam supply system

13. AVAILABILITY STATEMENT
unlimited

14. SECURITY CLASSIFICATION
(This Page)
unclassified
(This Report)
unclassified

15. NUMBER OF PAGES

16. PRICE

Federal Recycling Program

UNITED STATES
NUCLEAR REGULATORY COMMISSION
WASHINGTON, DC 20555-0001

OFFICIAL BUSINESS